Chapter IX. Magnetism:
Magnetic Properties of Solids from First-Principles

Summary: Magnetism is a vast subject. This three-hour lecture will merely touch upon some of the magnetic properties of solids which are accessible to *ab initio* calculations. Specifically, this lecture will cover spin-density functional theory, *ab initio* calculation of magnetic properties of solids at zero temperature, thermodynamical properties of magnets, effects of relativity in solids (spin-orbit coupling induced phenomena), magnetism in low-dimensional systems (surface and thin films).

Table of Contents of Chapter 9

9.1. Spin-Density Functional Theory

[von Barth, Hedin, J. Phys. C 5 (1972) 1629; Rajagopal, Callaway, PRB 1 (1973) 1912]

Consider a solid as a many-electron system in an external electric potential $V_{ext}(\mathbf{r})$ and an external magnetic field $\mathbf{B}_{ext}(\mathbf{r})$. For simplicity, $\mathbf{B}_{ext}(\mathbf{r}) = B_{ext}(\mathbf{r})\hat{z}$ is assumed. The system Hamiltonian is

$$\hat{H} = \hat{H}_{e,K} + \hat{H}_{e-e} + \hat{H}_{ext} \qquad (9.1.1)$$

$$\hat{H}_{e,K} = \sum_{i=1}^{N} -\frac{1}{2}\nabla_i^2$$ electron kinetic energy

$$\hat{H}_{e-e} = \frac{1}{2}\sum_{i\neq j}\sum_{j=1}^{N}\frac{1}{|\mathbf{r}_i - \mathbf{r}_j|}$$ electron-electron Coulomb interaction

$$\hat{H}_{ext} = -\sum_{i}^{N}\sum_{\alpha=1}^{M}\frac{Z_\alpha}{|\mathbf{r}_i - \mathbf{R}_\alpha|} + V_{field}(\mathbf{r}) + \sigma_z B(\mathbf{r})$$ electron-nuclei Coulomb interaction + applied fields

$$= V_{ext}(\mathbf{r}) + \sigma_z B(\mathbf{r}).$$

Electrons are fermions with ½ -spin, and thus their spins are either up (↑) (along z-axis) or down (↓) (against z-axis).

[In this way, we have ignored relativistic effects and diamagnetic effects]

Density functional (or Hohenberg-Kohn-Sham) theorems now read:

(1) The GS properties are a unique functional of both spin-up density $n_\uparrow(\mathbf{r})$ and spin-down density $n_\downarrow(\mathbf{r})$ for given $V_{\text{ext}}(\mathbf{r})$ and $\mathbf{B}_{\text{ext}}(\mathbf{r})$; the correct GS $n_{0\uparrow}(\mathbf{r})$ and $n_{0\downarrow}(\mathbf{r})$ minimize the energy functional $E[n_\uparrow(\mathbf{r}), n_\downarrow(\mathbf{r})]$ and this minimum is the GS energy E_0.

(2) The GS $n_\uparrow(\mathbf{r})$ and $n_\downarrow(\mathbf{r})$ can be obtained by solving selfconsistently a set of spin-dependent Kohn-Sham equations

$$\{-\frac{1}{2}\nabla^2 + V_{eff,\sigma}(\mathbf{r})\}\phi_{i,\sigma}(\mathbf{r}) = \varepsilon_{i,\sigma}\phi_{i,\sigma}(\mathbf{r}), \quad \sigma = \uparrow \text{ or } \downarrow \qquad (9.1.2)$$

$$n_\sigma(\mathbf{r}) = \sum_{i=1}^{N_\sigma} |\psi_{i,\sigma}(\mathbf{r})|^2, \quad V_{eff,\sigma}(\mathbf{r}) = V_{ext}(\mathbf{r}) + \sigma_z B(\mathbf{r}) + V_h(\mathbf{r}) + V_{xc,\sigma}(\mathbf{r}), \; N_\uparrow + N_\downarrow = N,$$

$$V_h(\mathbf{r}) = \int d\mathbf{r}' \frac{n(\mathbf{r}')}{|\mathbf{r}-\mathbf{r}'|}, \qquad V_{xc,\sigma}(\mathbf{r}) = \frac{\delta E_{xc}[n_\uparrow(\mathbf{r}), n_\downarrow(\mathbf{r})]}{\delta n_\sigma(\mathbf{r})}.$$

The number density is $n(\mathbf{r}) = (n_\uparrow(\mathbf{r}) + n_\downarrow(\mathbf{r}))$ and spin density is $m(\mathbf{r}) = (n_\uparrow(\mathbf{r}) - n_\downarrow(\mathbf{r}))$.

The total energy is given by

$$E = \sum_{\sigma} \sum_{i=1}^{N_\sigma} \varepsilon_{i,\sigma} - \frac{1}{2} \int d\mathbf{r} n(\mathbf{r}) V_h(\mathbf{r}) - \sum_{\sigma} \int d\mathbf{r} n_\sigma(\mathbf{r}) V_{xc,\sigma}(\mathbf{r}) + E_{xc}[n_\uparrow(\mathbf{r}), n_\downarrow(\mathbf{r})]. \quad (9.1.3)$$

(3) Local spin-density approximation

Assume

$$E_{xc}[n_\uparrow(\mathbf{r}), n_\downarrow(\mathbf{r})] \equiv \int n(\mathbf{r}) \varepsilon_{xc}[n_\uparrow(\mathbf{r}), n_\downarrow(\mathbf{r})] d\mathbf{r} \approx \int n(\mathbf{r}) \varepsilon_{xc}(n_\uparrow(\mathbf{r}), n_\downarrow(\mathbf{r})) d\mathbf{r} \quad (9.1.4)$$

where the exchange-correlation (x-c) energy per electron $\varepsilon_{xc}(n_\uparrow(\mathbf{r}), n_\downarrow(\mathbf{r}))$ is set to that of a spin-polarized homogeneous electron gas with the densities $n_\uparrow(\mathbf{r})$ and $n_\downarrow(\mathbf{r})$.

$$\varepsilon_{xc}^h(n_\uparrow(\mathbf{r}), n_\downarrow(\mathbf{r})) = \varepsilon_x^h(n_\uparrow(\mathbf{r}), n_\downarrow(\mathbf{r})) + \varepsilon_c^h(n_\uparrow(\mathbf{r}), n_\downarrow(\mathbf{r})), \quad (9.1.5)$$

where the exchange energy density per electron is

$$\varepsilon_x^h(n_\uparrow(\mathbf{r}), n_\downarrow(\mathbf{r})) = -3\left(\frac{3}{4\pi}\right)^{1/3} \frac{1}{n} (n_\uparrow^{4/3}(\mathbf{r}) + n_\downarrow^{4/3}(\mathbf{r})). \quad (9.1.6)$$

$\varepsilon_c^h(n_\uparrow(\mathbf{r}), n_\downarrow(\mathbf{r}))$ could be calculated by perturbational many-body theories (e.g., RPA) or by QMC.

(4) Spin-polarized GGA

$$E_{xc}[n_\uparrow(\mathbf{r}), n_\downarrow(\mathbf{r})] \approx \int f(n_\uparrow(\mathbf{r}), n_\downarrow(\mathbf{r}), \nabla n_\uparrow(\mathbf{r}), \nabla n_\downarrow(\mathbf{r}))d\mathbf{r} \qquad (9.1.7)$$

GGA functionals $f(n_\uparrow(\mathbf{r}), n_\downarrow(\mathbf{r}), \nabla n_\uparrow(\mathbf{r}), \nabla n_\downarrow(\mathbf{r}))$ were constructed under guidances of wave vector analysis of x-c energy functional and were forced to have the same physical asymptotic behaviors such as x-c sum rule [Perdew, et al., PRL 77 (1996) 3865].

A classic example of successful GGA is that GGA predicts the correct ground state (FM BCC) for Fe whilst LDA predicts a wrong ground state (NM FCC) for Fe [see, e.g., Guo, Wang, CJP 949 (2000) 949].

9.2. Magnetic properties of solids at zero temperature

(1) Common magnetic structures

(a) Ferromagnets

bcc Fe, hcp Co, fcc Ni, CrO_2

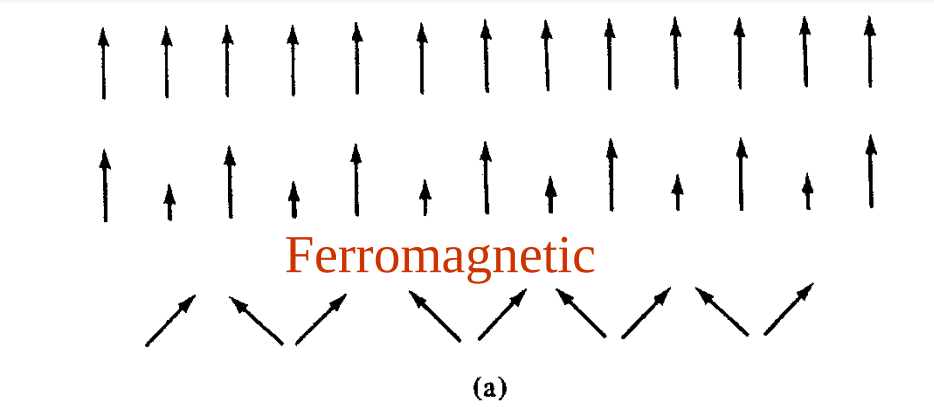

(b) Anti-ferromagnets

bcc Cr, MnO, NiO, La_2CuO_4

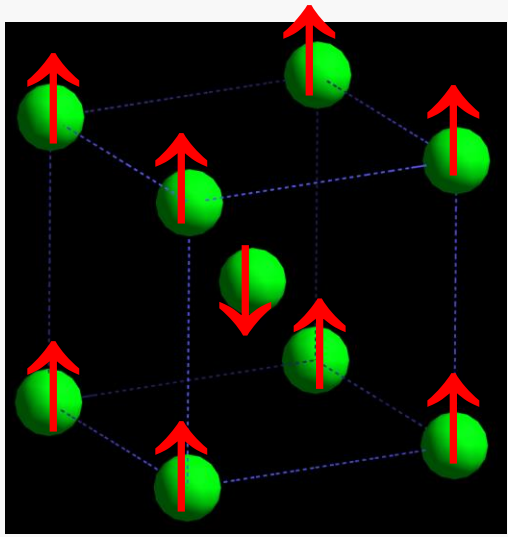

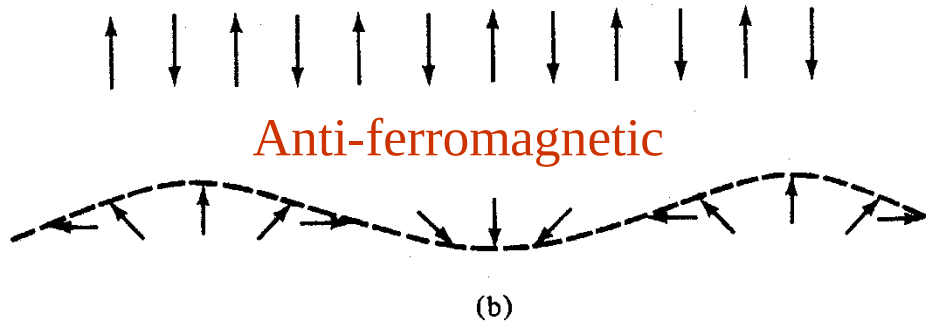

(c) Ferrimagnets

Fe_3O_4, Sr_2FeMoO_6

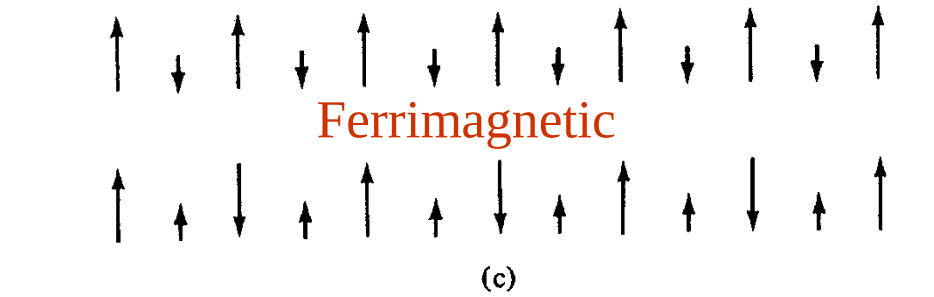

(2) *Ab initio* determination of GS and metastable state magnetic structures

(a) Phase diagram of Fe

LDA calculations for Fe

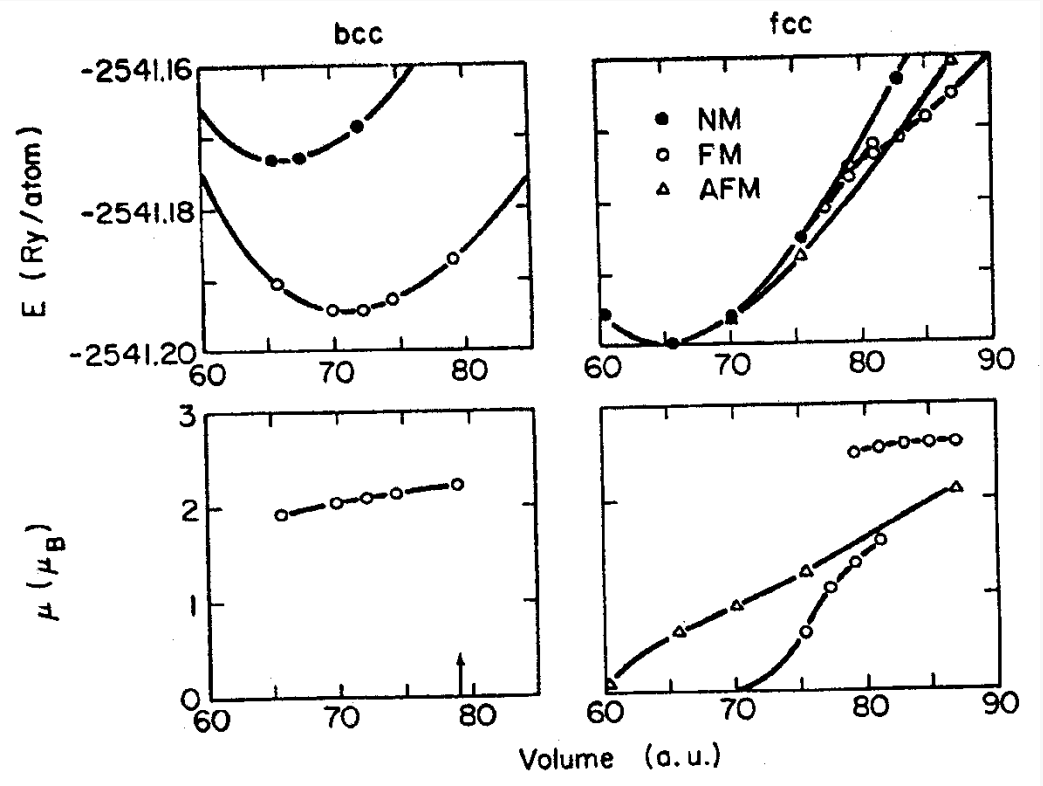

[Wang, et al., PRL 54 (1985) 1852]

GGA calculations for Fe

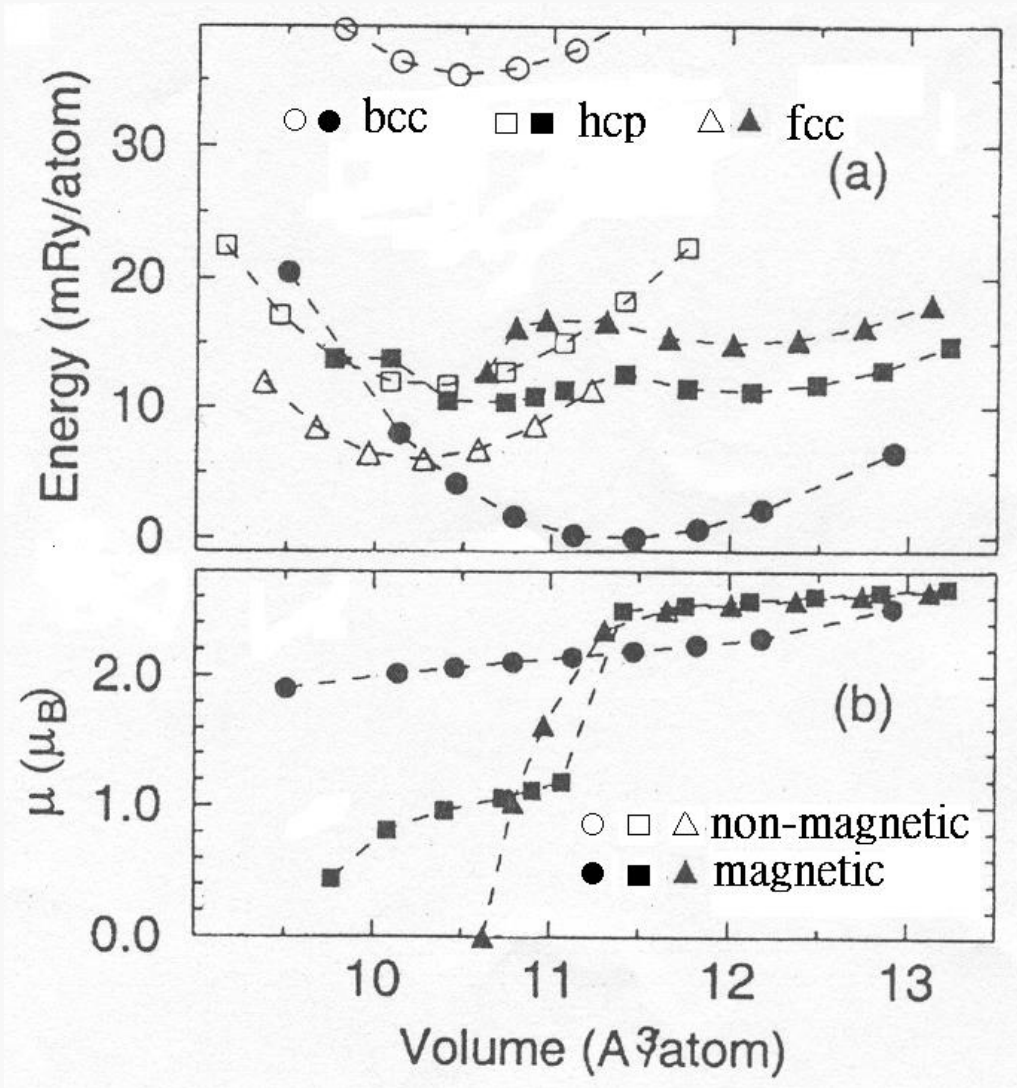

[Guo, Wang, Chin. J. Phys. 38 (2000) 949]

Fe ground state:

LDA: NM fcc (wrong);

GGA: FM bcc (correct).

(b) Metastable and unstable structures

[Guo, Wang, Chin. J. Phys. 38 (2000) 949]

Lattice constants and elastic constants of bcc, fcc and hcp Fe

Note that NM bcc, FM fcc and FM hcp structures have negative elastic constants, and thus they are unstable under shear strains.

bcc Fe	a_0	V_0	B	C'	C_{11}	C_{12}	C_{44}	m_s	E_0
	Å	Å^3/atom	Mbar	Mbar	Mbar	Mbar	Mbar	μ_B	Ry/atom
FM	2.84	11.40	1.86	0.69	2.79	1.40	0.99	2.17	-2545.6107
Exp[a]	2.87	11.82	1.72	0.48	2.32	1.36	1.17	2.22	
NM	2.76	10.52	2.76	-1.10	1.30	3.49	1.41		-2545.5754

(b)

fcc Fe	a_0	V_0	B	C'	C_{11}	C_{12}	C_{44}	m_s	E_0
	Å	Å^3/atom	Mbar	Mbar	Mbar	Mbar	Mbar	μ_B	Ry/atom
FM	3.63	11.97	1.82	-0.77	0.79	2.33	0.23	2.55	-2545.5902
NM	3.45	10.30	3.17	1.25	4.84	2.34	2.87		-2545.5908

(c)

hcp	a_0	c/a	V_0	B	$C_{11}+C_{12}$	$C_{11}-C_{12}$	C_{11}	C_{12}	C_{13}	C_{33}	C_{55}	m_s
Fe	Å		Å^3/atom	Mbar	Mbar	Mbar	Mbar	Mbar	Mbar	Mbar	Mbar	μ_B
FM	2.52	1.732	12.04	1.56	4.17	-0.29	1.94	2.23	0.87	3.14	-0.62	2.54
NM	2.46	1.586	10.23	2.97	7.27	3.85	5.56	1.71	1.43	6.47	2.48	
Exp[b]			8.89		9.40	3.40	6.40	3.00	2.55	6.50	4.20	

Phonon band structure of bcc Fe
[Hsueh, et al., PRB 66 (2002) 52420]

Note that both NM and FM with a reduced spin moment have negative (imaginary) phonon frequencies and thus they are dynamically unstable. In this case, bcc structure is stabulized by ferromagnetism. In other cases, magnetism can de-stabulize a structure (e.g., Fe in fcc and hcp structures). Clearly, magnetism play a role in structural stability.

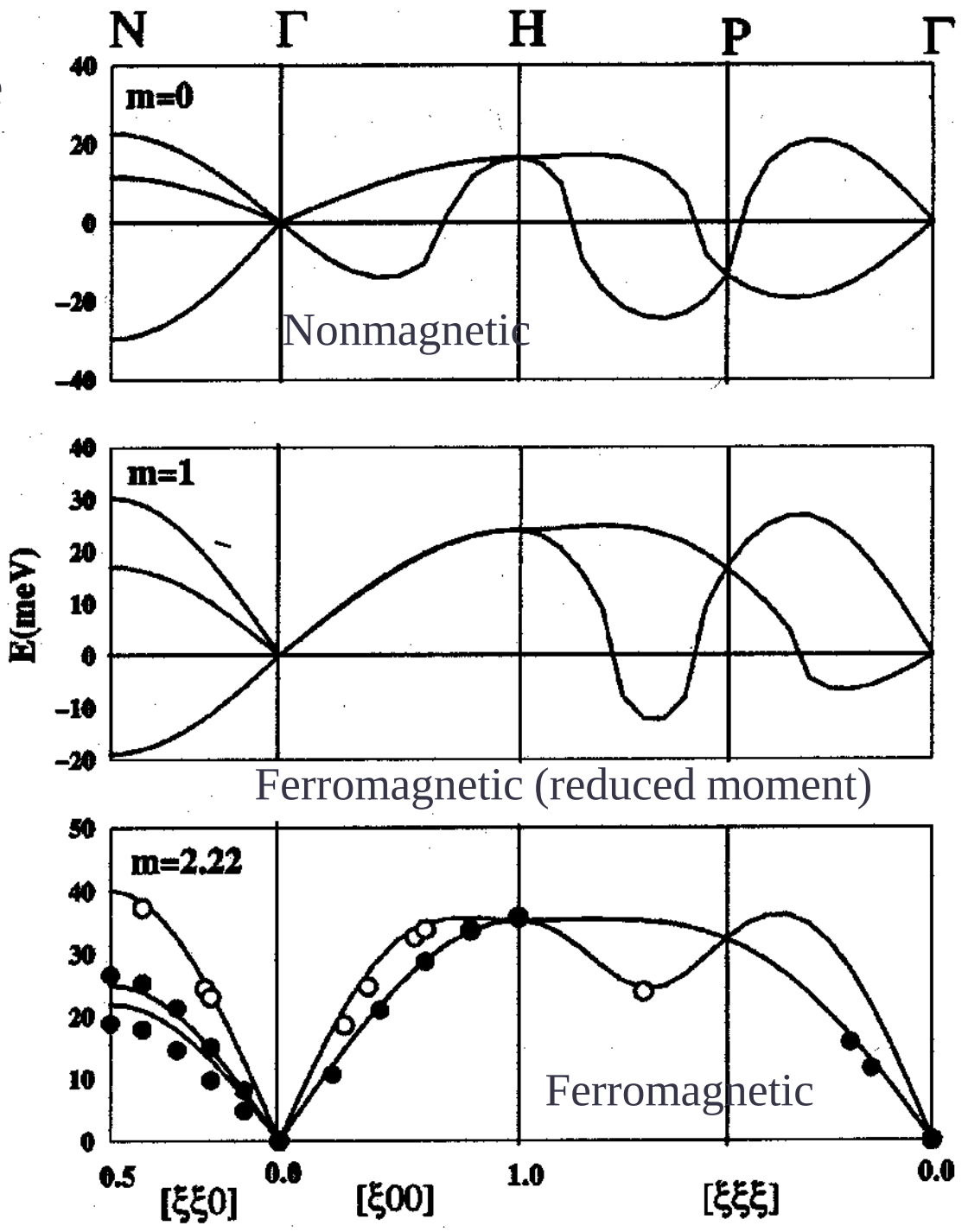

(3) Magnetization
(magnetic moments)

Total (spin) magnetization

$$M = \int_{\Omega} d\mathbf{r} m(\mathbf{r}) \qquad [\mu_B / \text{cell}].$$

Local (atom-decomposed) magnetic moment

$$M_i = \int_{\Omega_i} d\mathbf{r} m(\mathbf{r}) \qquad [\mu_B / \text{atom}].$$

Spin-polarized DFT (LSDA) calculations for metallic alloys ($A_{1-c}B_c$)

($Z_V = 23$, $Z_{Fe} = 26$, $Z_{Ni} = 28$)

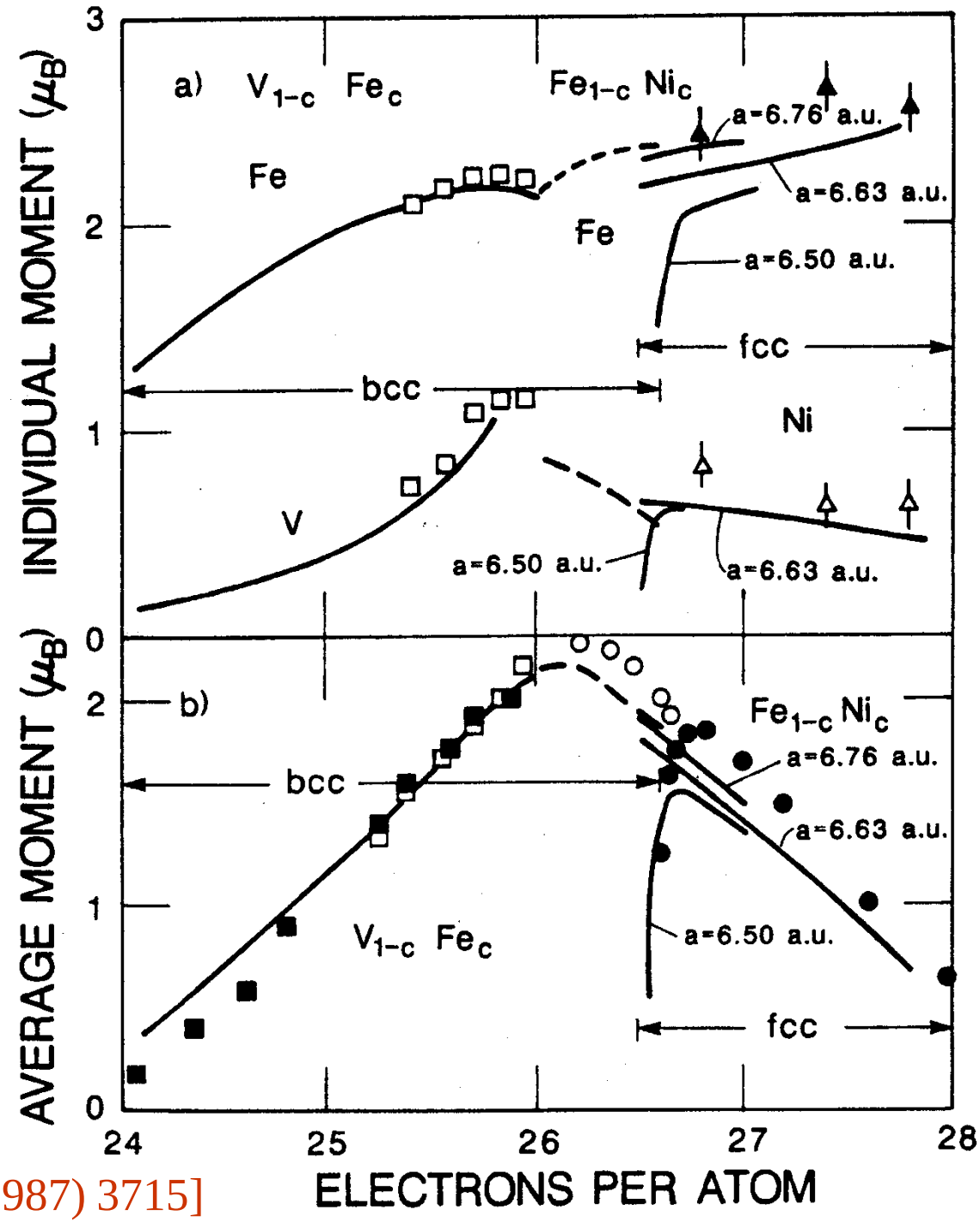

[Johnson, et al., JAP 61 (1987) 3715]

(4) Electronic structure (Band structure and density of states)

(a) Nonmagnetic and ferromagnetic cases

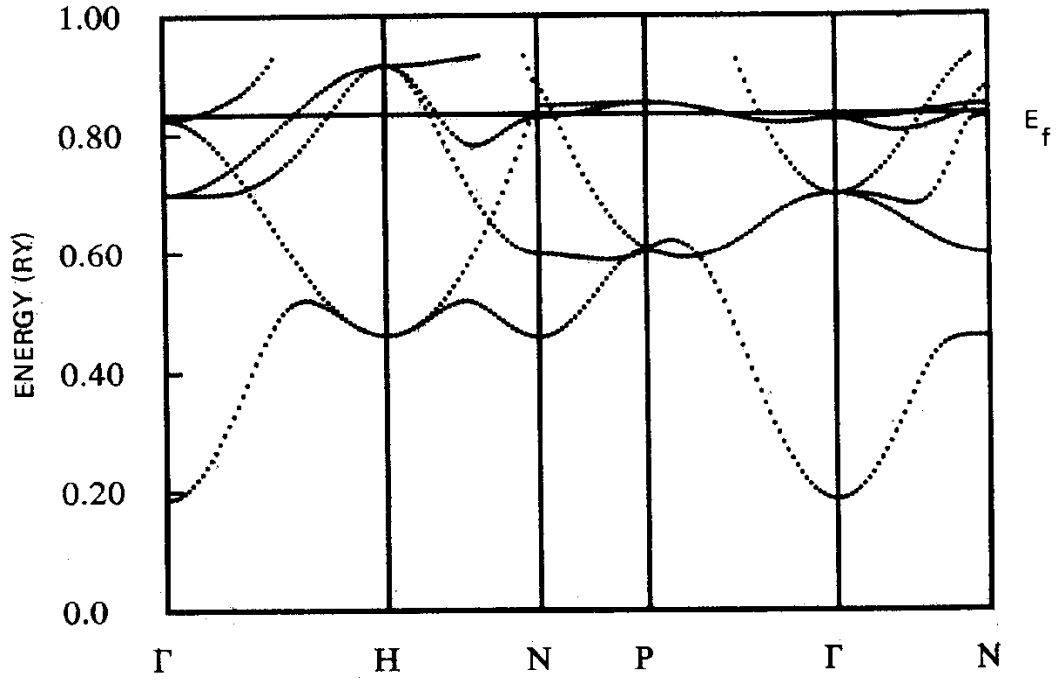

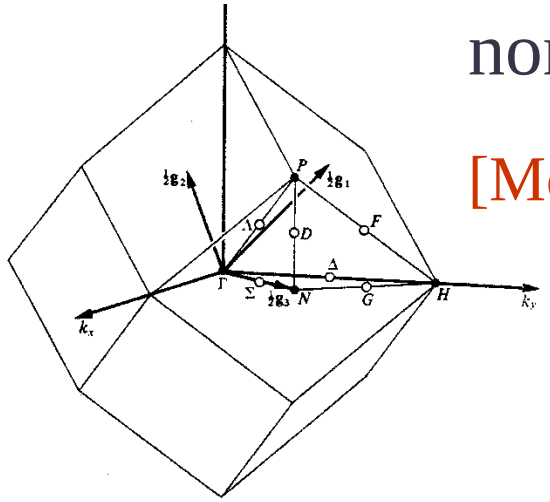

nonmagnetic

[Moruzzi, et al., 1978]

Band structure of bcc Fe

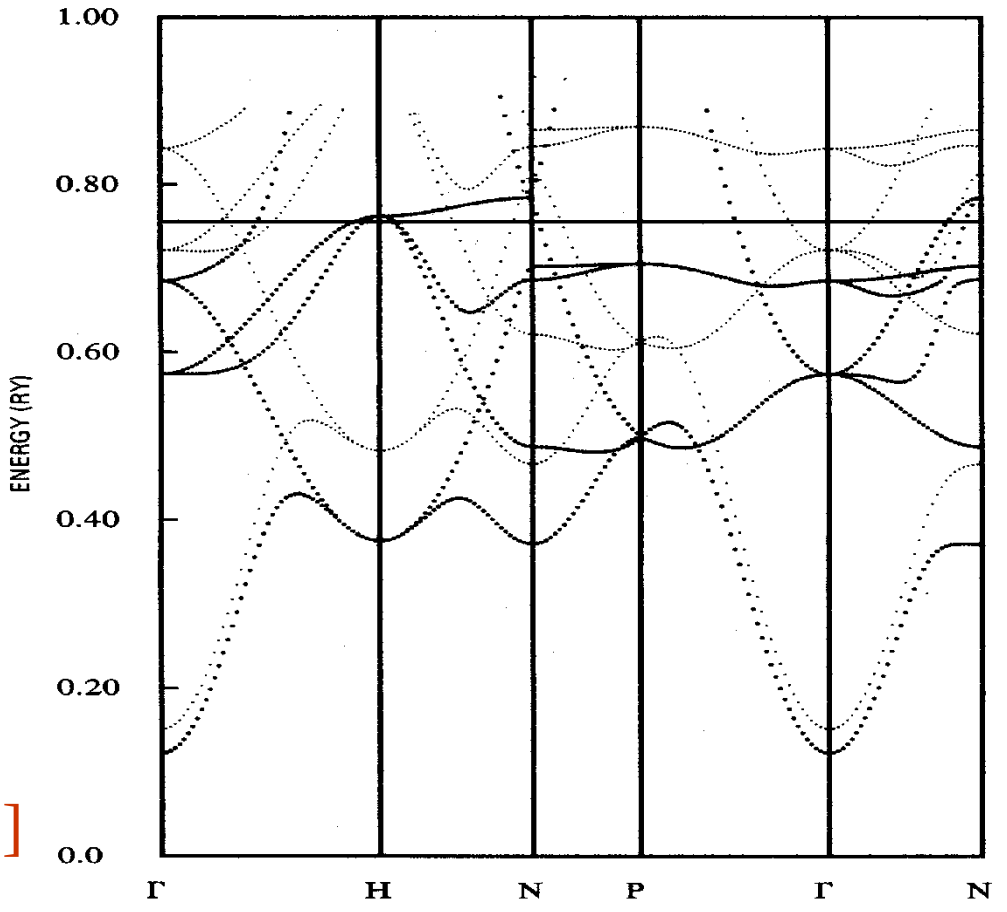

ferromagnetic

Density of states of bcc Fe

[Moruzzi, et al., 1978]

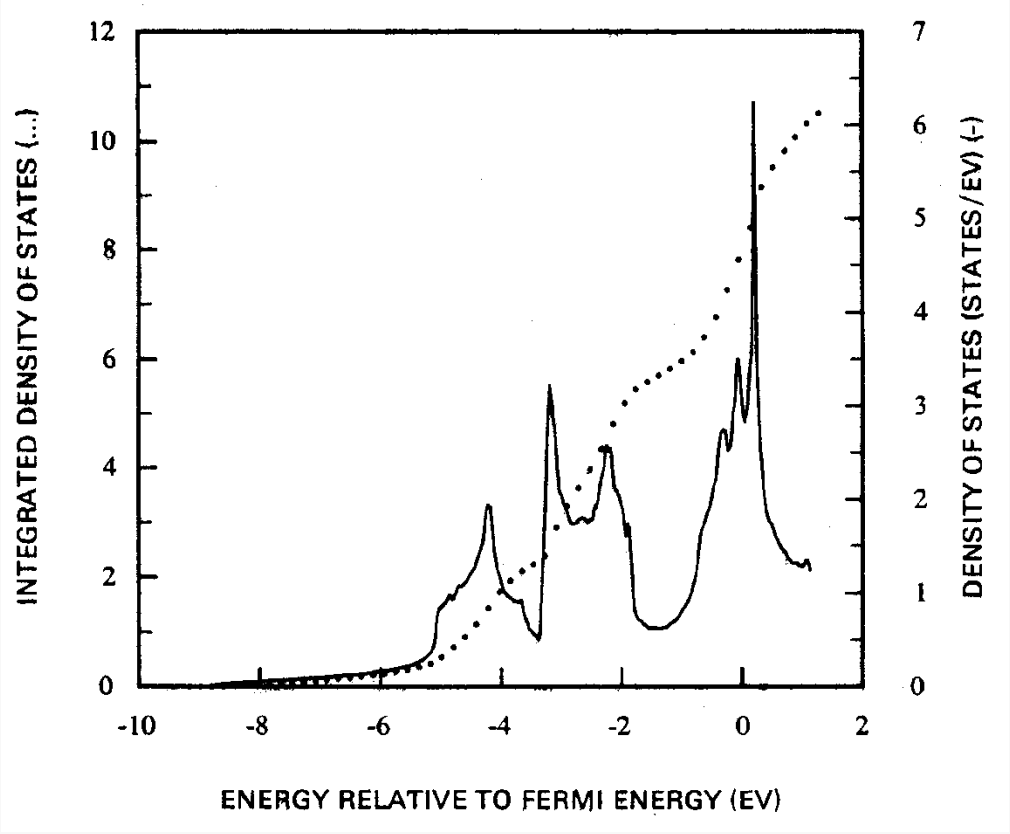

nonmagnetic

[$N(E_F)$ = 3.1 states/eV/atom]

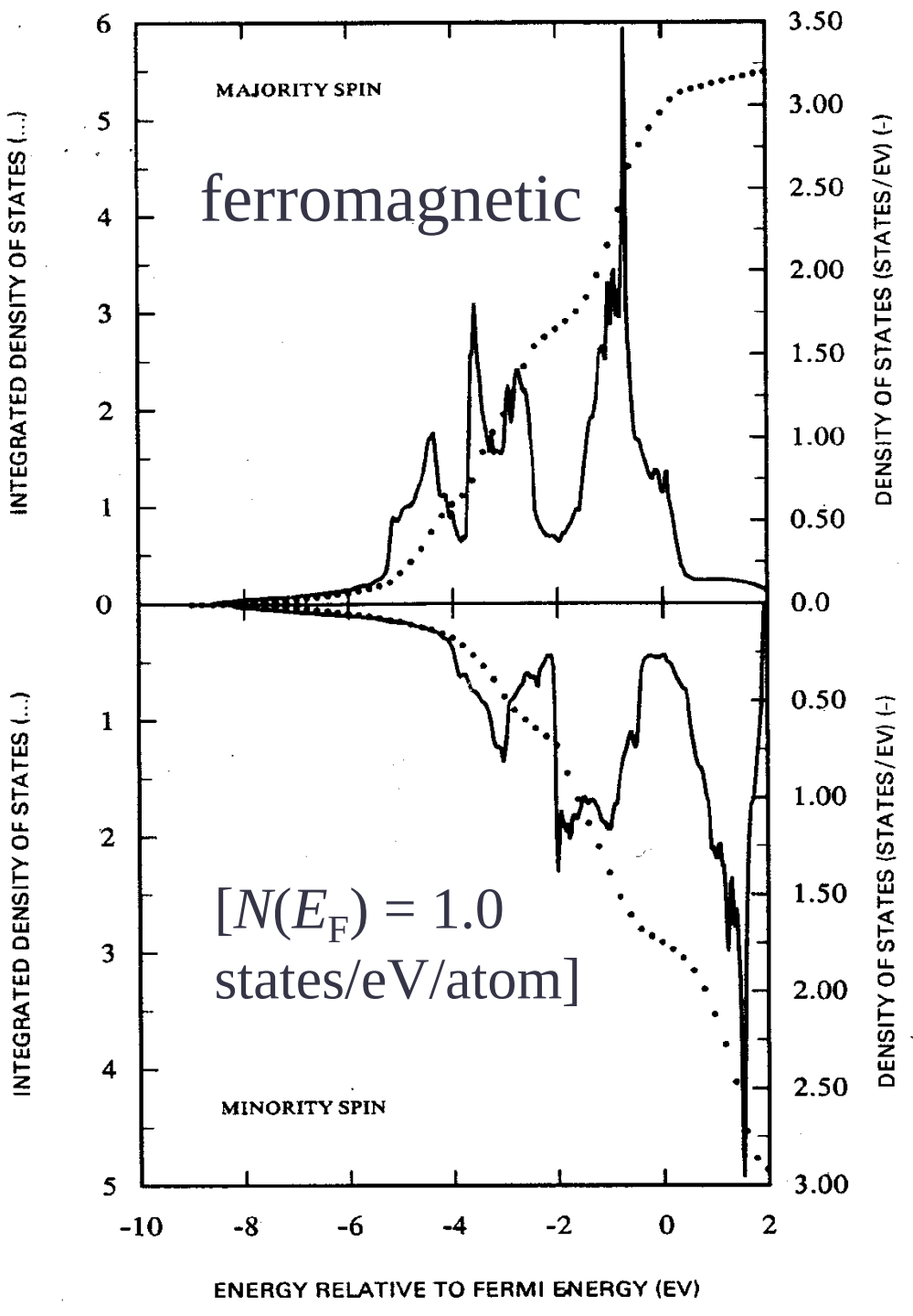

ferromagnetic

[$N(E_F)$ = 1.0 states/eV/atom]

Band structure of fcc Ni

Nonmagnetic

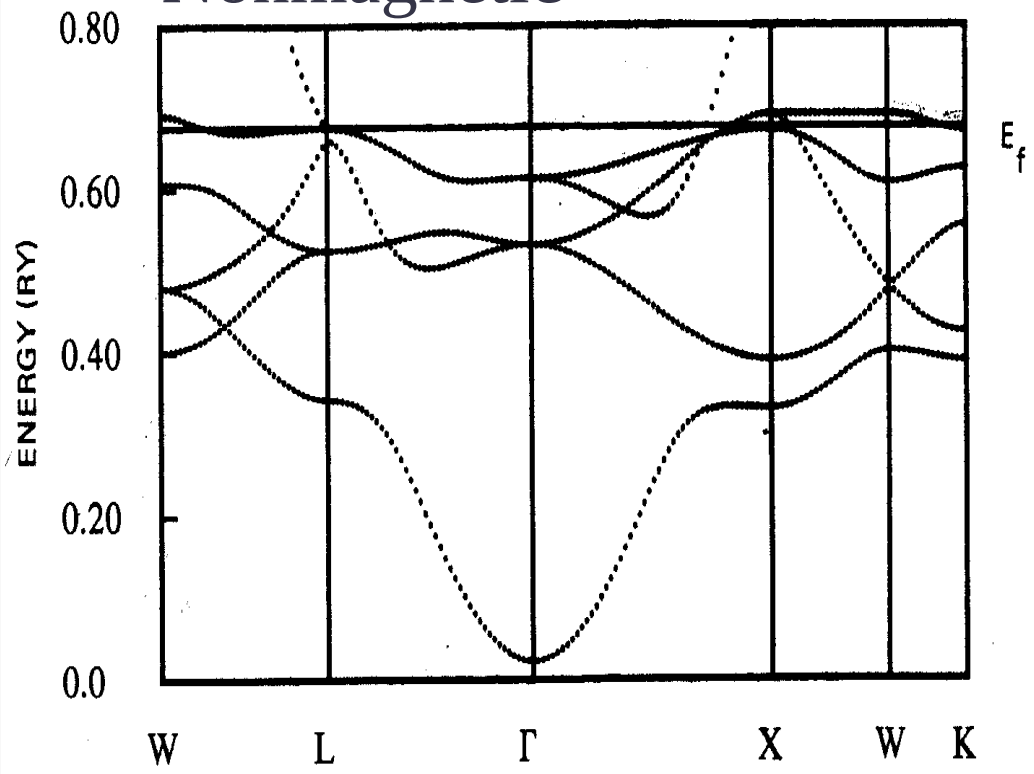

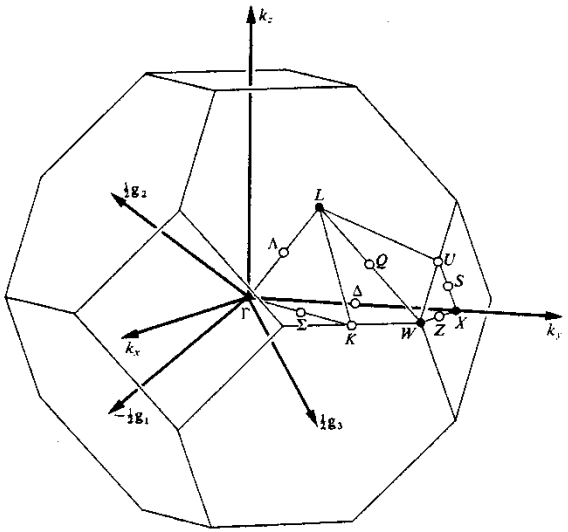

Ferromagnetic

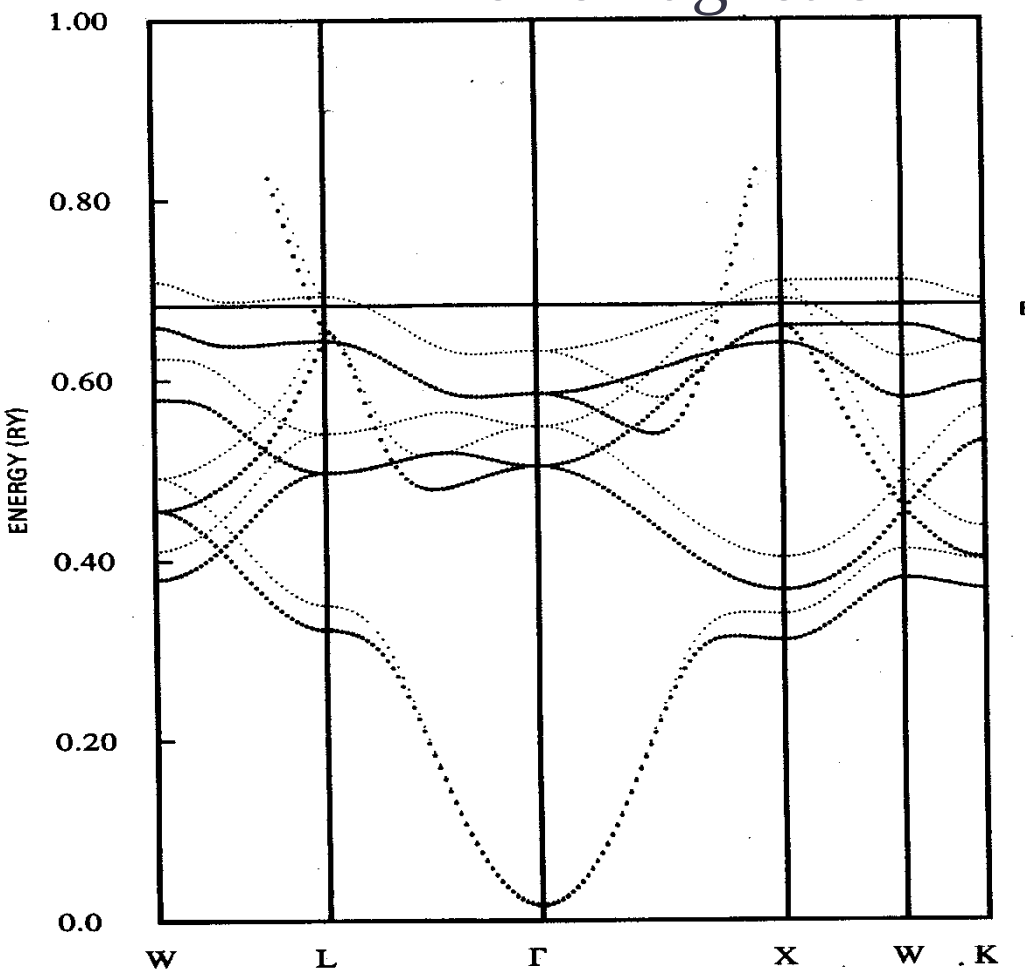

Dark points for majority spin, light points for minority spin.

[Moruzzi, et al., 1978]

Density of states of fcc Ni

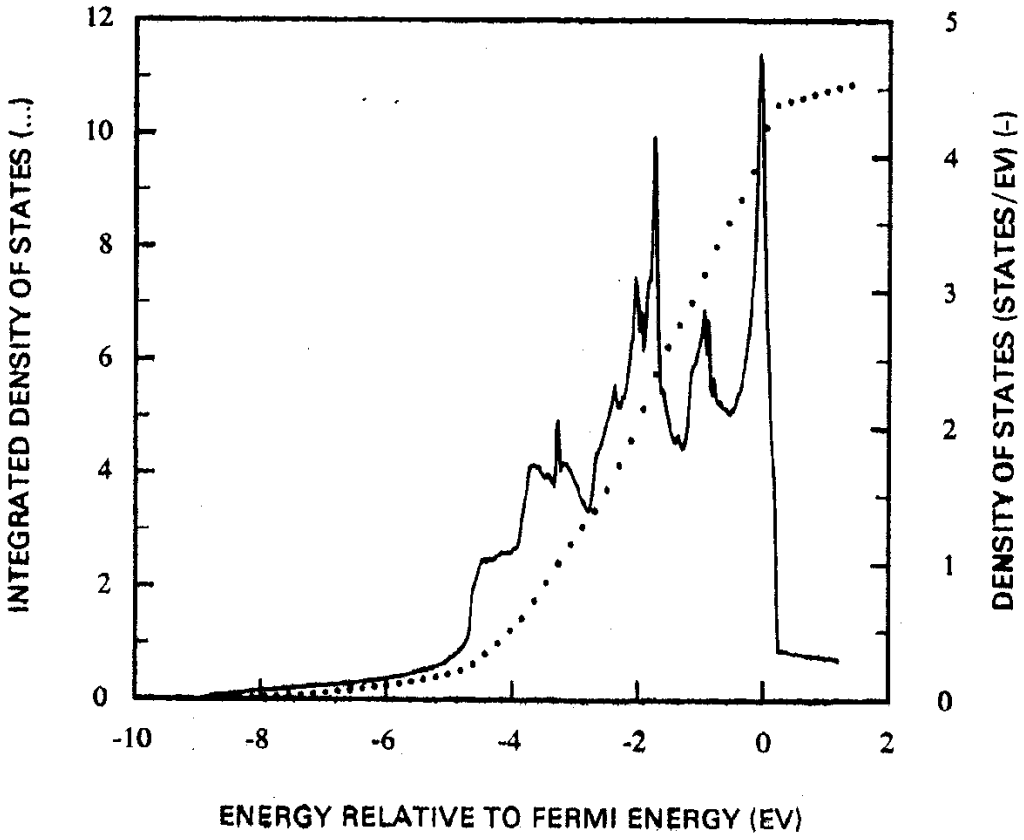

Nonmagnetic

[$N(E_F)$ = 4.1 states/eV/atom]

Ferromagnetic

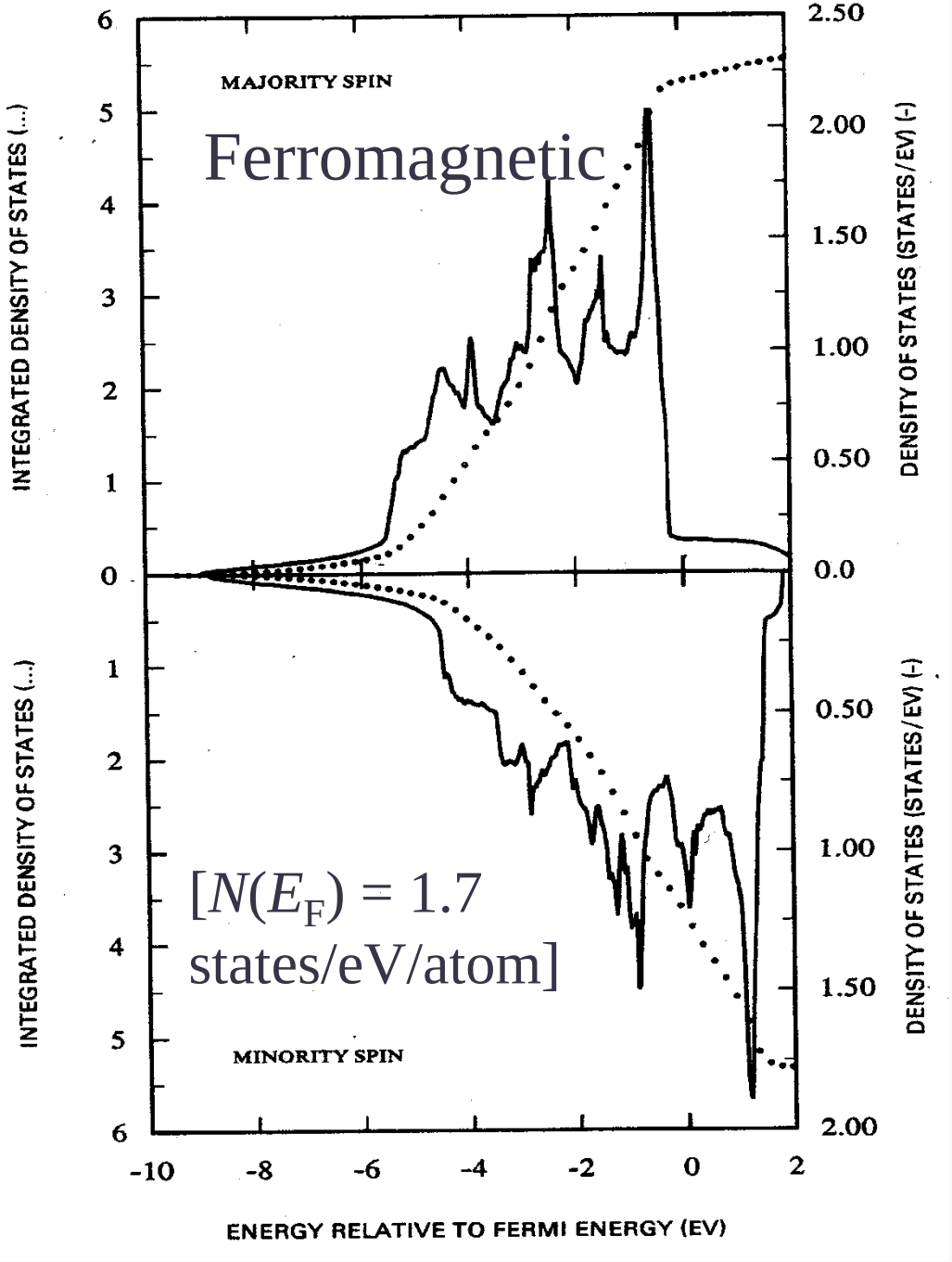

[$N(E_F)$ = 1.7 states/eV/atom]

[Moruzzi, et al., 1978]

(b) Antiferromagnetic case

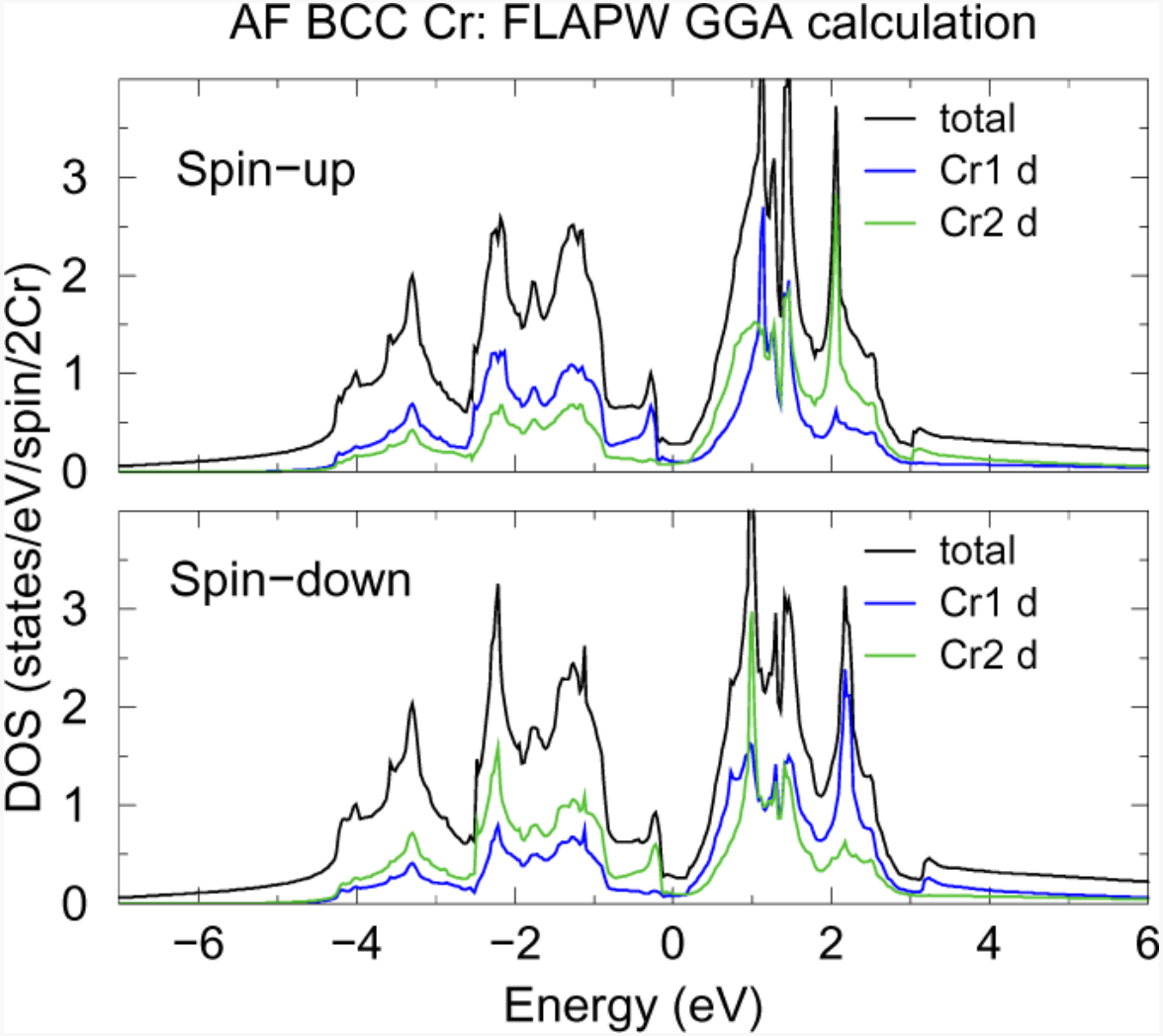

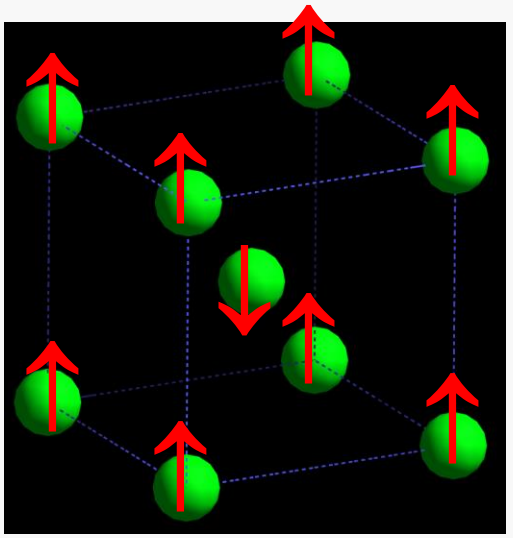

(5) Stoner criterion [Janak, PRB 16 (1977) 255]

Why are Fe, Co and Ni ferromagnetic whilst the others are not? Starting with a LDA nonmagnetic band structure and working within linear response theory, one can find that the magnetic susceptibility is

$$\chi = \frac{N(\varepsilon_F)}{1 - IN(\varepsilon_F)}, N(\varepsilon_F) = \sum_i \delta(\varepsilon_F - \varepsilon_i), \qquad (9.2.1)$$

$$I = \int \gamma(\mathbf{r})[-\frac{\partial^2}{\partial m^2} n\varepsilon_{xc}(n,m)]d\mathbf{r}, \gamma(\mathbf{r}) = \sum_i \frac{\delta(\varepsilon_F - \varepsilon_i)|\varphi_i|^2}{N(\varepsilon_F)}$$

where $N(\varepsilon_F)$ is the density of state at the ε_F and I the Stoner exchange constant.

Thus, if $I\,N(\varepsilon_F) \geq 1$, $\chi = \infty$ or < 0. This means that the system is ferromagnetically unstable, i.e., ferromagnetism would occur.

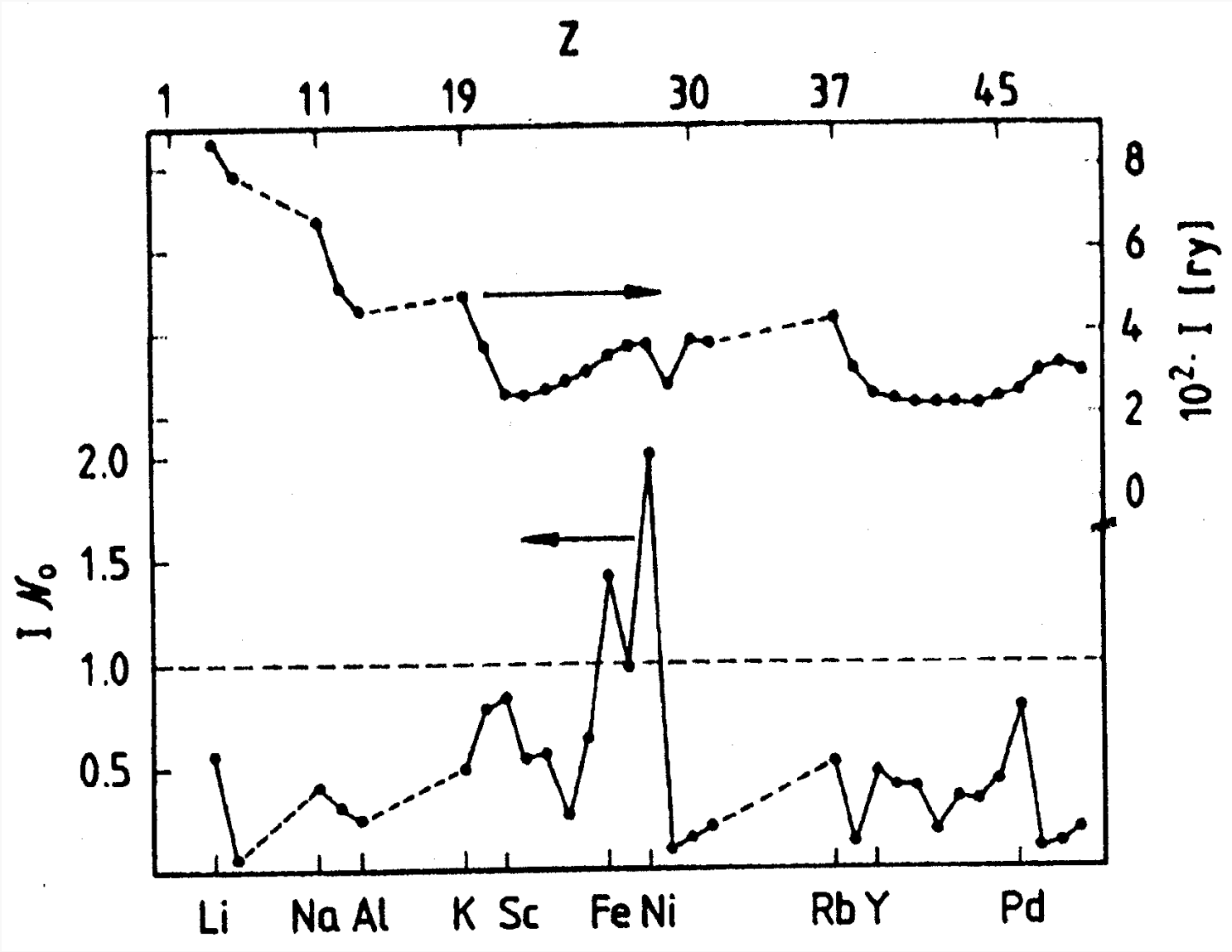

[Janak, PRB 16 (1977) 255]

3. Thermodynamical properties and transition temperature

(1) Thermodynamic ($T \neq 0$) DFT [Mermin, PR 137 (1965) A1441]

Consider a many electron system in equilibrium with a heat and particles reserviour (T and μ) (*i.e.*, the grand canonical ensemble). By definition, the grand potential at equilibrium is

$$\Omega = Tr\{\rho(\hat{H} - \mu\hat{N} + \frac{1}{\beta}\ln\rho)\}, \qquad (\beta = \frac{1}{kT}) \tag{9.3.1}$$

$$n(\mathbf{r}) = Tr\{\rho\hat{n}(\mathbf{r})\}, \qquad \hat{n}(\mathbf{r}) = \sum_{i=1}^{N}\delta(\mathbf{r}-\mathbf{r}_i) \tag{9.3.2}$$

$$\rho = \frac{e^{-\beta(H-\mu N)}}{Tr\{e^{-\beta(H-\mu N)}\}} \tag{9.3.3}$$

Hohenberg-Kohn theorem: the ensemble-averaged density $n_0(\mathbf{r})$ minimizes the functional $\Omega[n] = F[n] + \int [V_{ext}(\mathbf{r}) - \mu]n(\mathbf{r})d\mathbf{r}$ where

$F[n]$ is a universal functional of $n(\mathbf{r})$.

The Kohn-Sham equ's for $T \neq 0$ are

$$[-\frac{1}{2}\nabla^2 + V_{eff}(\mathbf{r}) - \mu]\varphi_i(\mathbf{r}) = \varepsilon_i \varphi_i(\mathbf{r}) \qquad (9.3.4)$$

$$n(\mathbf{r}) = \sum_{i=1}^{N} |\varphi_i(\mathbf{r})|^2 \quad f(\varepsilon_i - \mu) \qquad (9.3.5)$$

(Fermi function)

$$V_{eff}(\mathbf{r}) = V_{ext}(\mathbf{r}) + \int \frac{n(\mathbf{r})}{|\mathbf{r}-\mathbf{r}'|} dr' + \frac{\delta F_{xc}[n]}{\delta n} \qquad (9.3.6)$$

where $F_{xc}[n]$ is defined by

$$\Omega[n(\mathbf{r})] = T_s[n(\mathbf{r})] - TS_s[n(\mathbf{r})] + \frac{1}{2}\int \frac{n(\mathbf{r})n(\mathbf{r}')}{|\mathbf{r}-\mathbf{r}|} d\mathbf{r}d\mathbf{r}' + F_{xc}[n(\mathbf{r})] + \int n(\mathbf{r})V_{ext}(\mathbf{r})d\mathbf{r} \qquad (9.3.7)$$

(entropy of non-interacting electrons)

$F_{xc}[n]$ is not known and it is not even clear how good a LDA will be, as $F_{xc}[n]$ has not been calculated reliably for jellium.

No $T \neq 0$ LDA calculations has been done for a real solid and the thermodynamic properties of a solid are often derived from $T = 0$ LDA calculations.

In principle, to calculate the thermodynamical properties and phase transition temperature, one should start with $T \neq 0$ spin-density functional theory of Mermin. However, so far such calculations have not been possible.

Nonetheless, it has been possible to accurately calculate these properties from first-principles indirectly.

(1) *Ab initio* Heisenberg model and Monte Carlo simulation

Heisenberg model $$H = -\frac{1}{2}\sum_{i}\sum_{j(\neq i)} J_{ij}\mathbf{S}_i\cdot\mathbf{S}_j. \qquad (9.3.8)$$

If exchange coupling parameters J_{ij} are known, one can easily calculate thermodynamical properties [e.g., *C(T)*, *M(T)*] via (classical) Monte Carlo simulation. Now the J_{ij}'s can be determined by mapping the calculated total energies for various magnetic configurations (structures) onto the Heisenber-like Hamiltonian

$$E_T = E_{PM} - \sum_i E_M - \frac{1}{2}\sum_{i,j} J_{r(ij)}\boldsymbol{\sigma}_i\cdot\boldsymbol{\sigma}_j. \qquad (9.3.9)$$

	E_m (mRy)	J_1 (mRy)	J_2 (mRy)	J_3 (mRy)
bcc Fe	25.1	4.209	1.648	-1.057

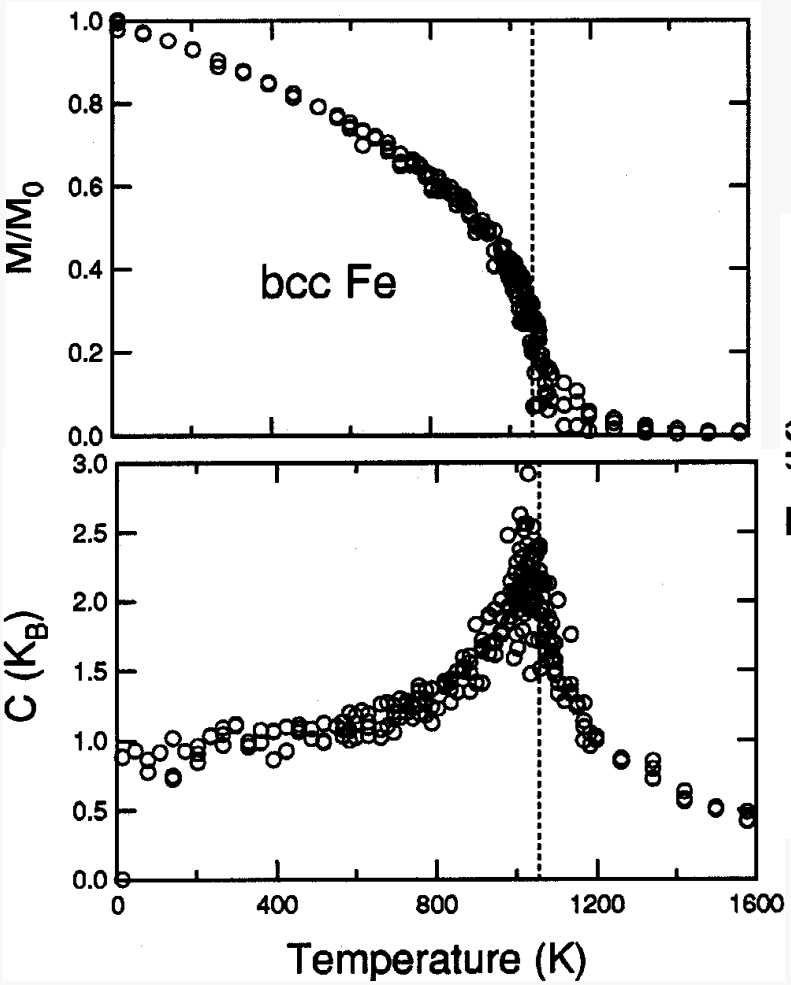

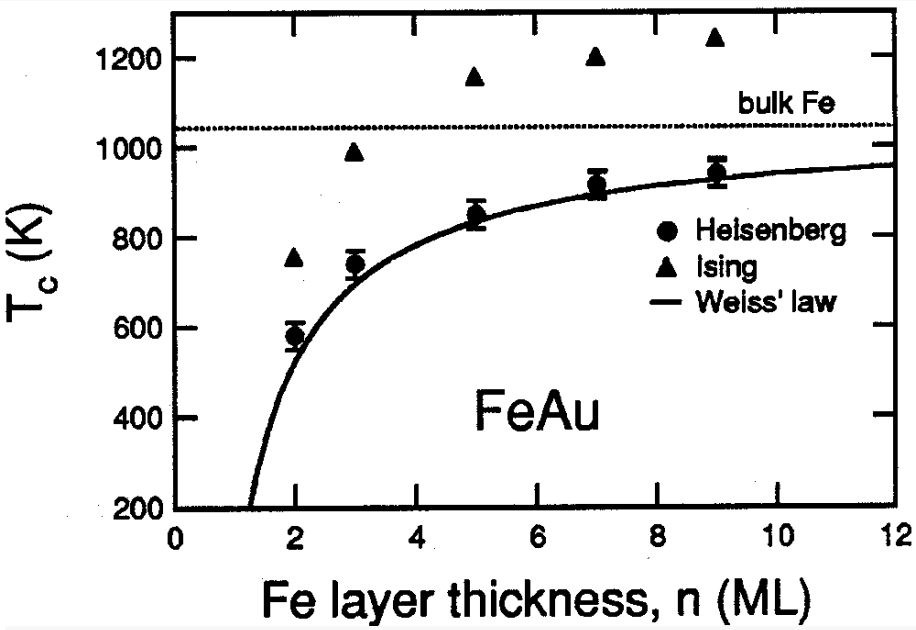

[PRB 62, 3354 (2000)]

(2) Spin-wave excitation, mean field theory and random phase approximation

Schematic of a transverse spin-wave

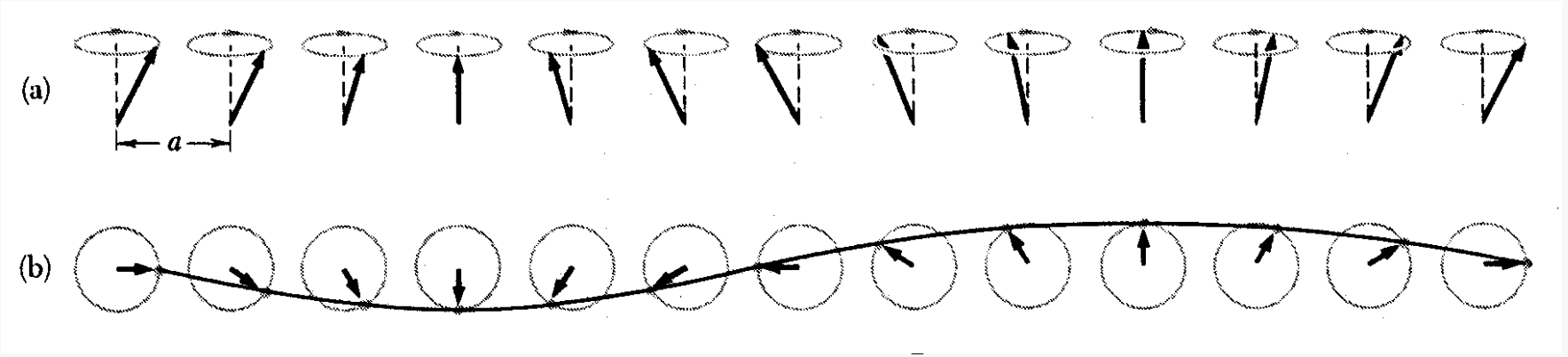

Presently, spin-wave excitation energies can be obtained either by Fourier transformation of the real-space exchange coupling constant $J_{ij}(r)$ or by frozen magnon (adiabetic spin-dynamics).

Spin-wave dispersion relation
(Magnon band structure)

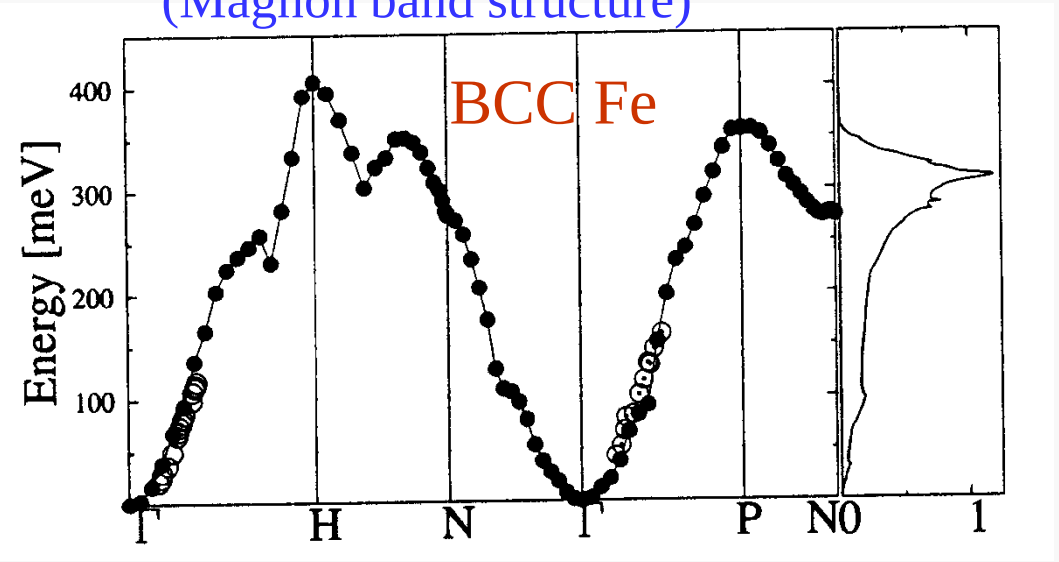

[Halilov, et al., PRB 58, 293 (1998)]

Once the magnon band structure is known, the transition temperature can be obtained on the RPA level as

$$\frac{1}{k_B T_c^{RPA}} = \frac{6\mu_B}{m}\frac{1}{N}\sum_{\mathbf{q}}\frac{1}{\hbar\omega_{\mathbf{q}}}. \qquad (9.3.10)$$

	T_c^{exp} (K)	T_c^{Stoner} (K)	T_c^{RPA} (K)
bcc Fe	1039	5300	1316
fcc Co	1390	4000	1558
fcc Ni	630	2900	642

[Halilov, et al., PRB 58, 293 (1998)]

3*d* transition metal linear atomic chains

[Tung and Guo, PRB 83, 144403 (2011)]

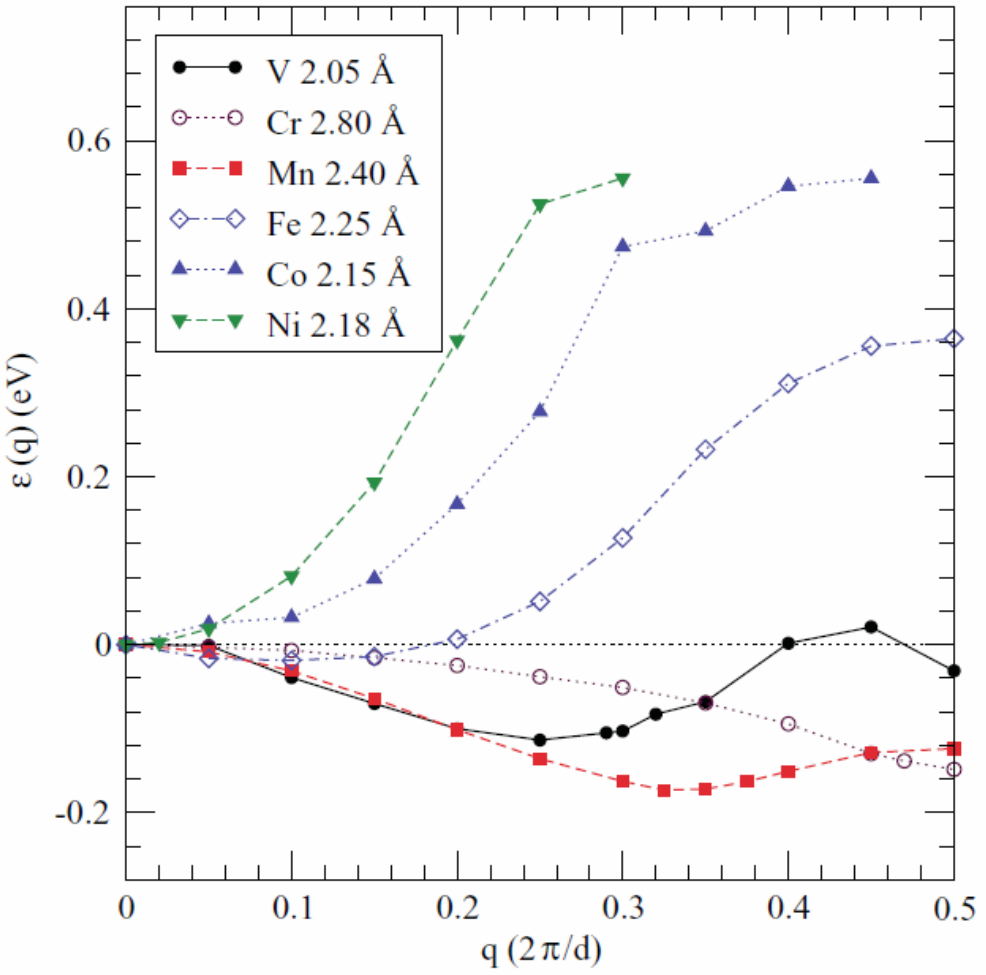

FIG. 2. (Color online) Calculated spin-wave energy spectra $\varepsilon(q)$ [i.e., magnon dispersion relations $\hbar\omega(q)$] of the 3*d* transition metal atomic chains at the ground-state bond length except the Cr chain where the bond length $d = 2.80$ Å is used.

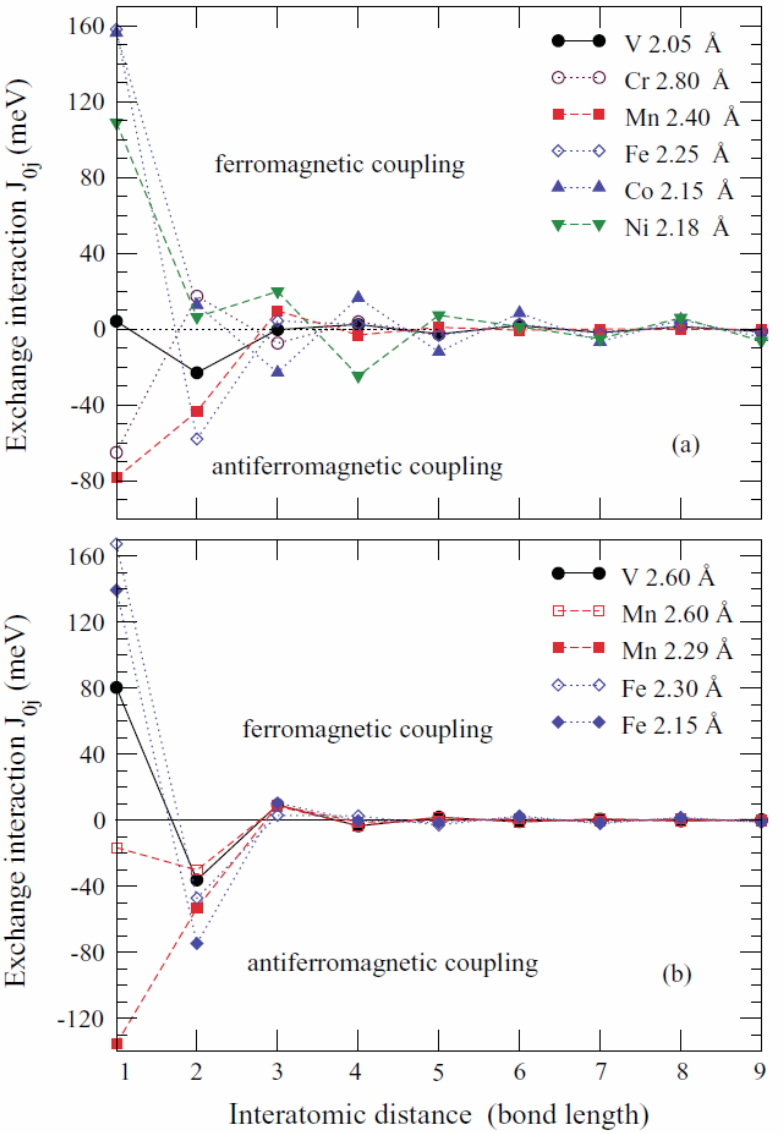

FIG. 3. (Color online) Calculated exchange-interaction parameters J_{0j} vs interatomic distance for the 3*d* transition metal chains with different bond lengths as labeled. In (a), the atomic chains are in their respective ground-state bond lengths except the Cr chain where the bond length $d = 2.80$ Å is used, and in (b), the atomic chains are in either stretched or compressed bond lengths.

TABLE II. Calculated exchange-interaction parameters (J_{0j}) (meV) between two jth near neighbors ($j = 1,2,3,4,5$) in the V, Cr, Mn, Fe, Co, and Ni atomic chains.

	J_{01}	J_{02}	J_{03}	J_{04}	J_{05}
V	4.2	−22.8	−0.2	2.6	−2.4
Cr	−65.0	17.6	−7.2	4.0	−2.6
Mn	−78.4	−43.2	9.8	−3.0	1.2
Fe	158.2	−57.8	4.4	2.6	−3.2
Co	156.4	13.0	−22.8	16.6	−11.8
Ni	109.0	6.6	20.0	−24.6	7.4

[Tung and Guo, PRB 83, 144403 (2011)]

TABLE III. Calculated spin-wave stiffness constant D (meVÅ^2) and magnetic transition temperature T_C of the 3d metal chains. Also listed are the D's and T_C's for the 3D and 2D metal systems from previous *ab initio* calculations and experimental measurements for comparison.

	Stiffness D			T_C (K)		
	3D	2D	1D	3D	2D	1D
V			−424			94
Cr			−106	311[g]		414
Mn			−504			274
Fe	250,[a] 330[b]	164[c]	−78	1414,[a] 1043[d]	1265[c]	410
Co	663,[a] 510[b]	570[c], 427[e]	616	1645,[a] 1388[d]	1300[c]	606
Ni	756,[a] 555[f]		656	397,[a] 627[d]		458

[a]Theoretical calculations (Ref. 18).
[b]Neutron-scattering measurement extrapolated to 0 K (Ref. 45).
[c]Theoretical calculations (Ref. 11).
[d]Experimental measurements (Ref. 46).
[e]Brillouin light-scattering measurement (Ref. 47).
[f]Neutron-scattering measurement (Ref. 48).
[g]Neutron-scattering measurement (Ref. 49).

[Tung and Guo, PRB 83, 144403 (2011)]

9.4. Relativistic Effects in Solids

(1) Effects of relativity in solids

We could actually see and hear relativity at work in daily life. For example, (a) the color of gold, and (b) components of a Hi-Fi system.

(a) Color and nobility of gold depend on relativity

Gold

silver

no relativity

=========>

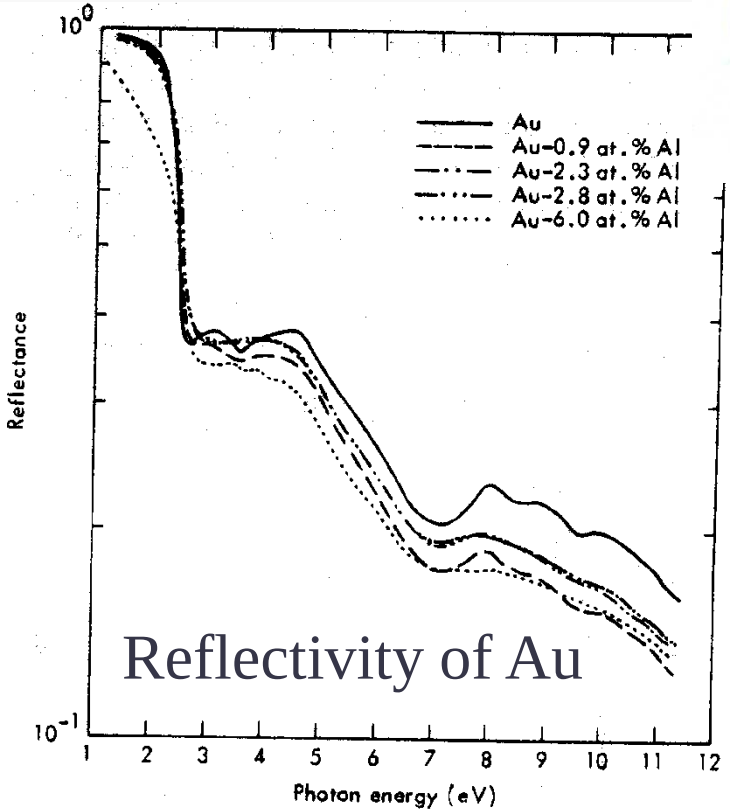

Reflectivity of Au

Ab initio calculations: Au surface becomes quite active without relativity.

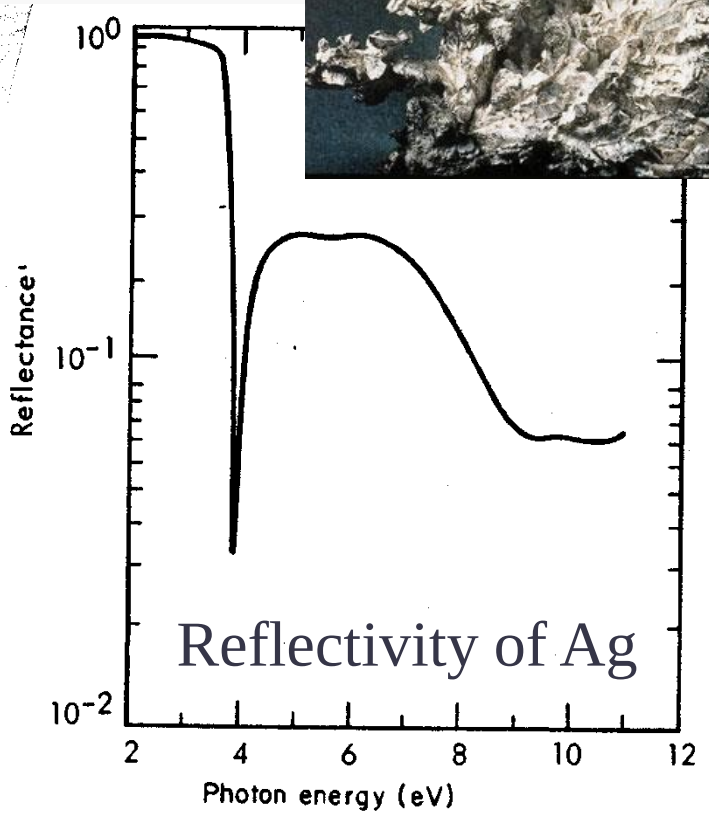

Reflectivity of Ag

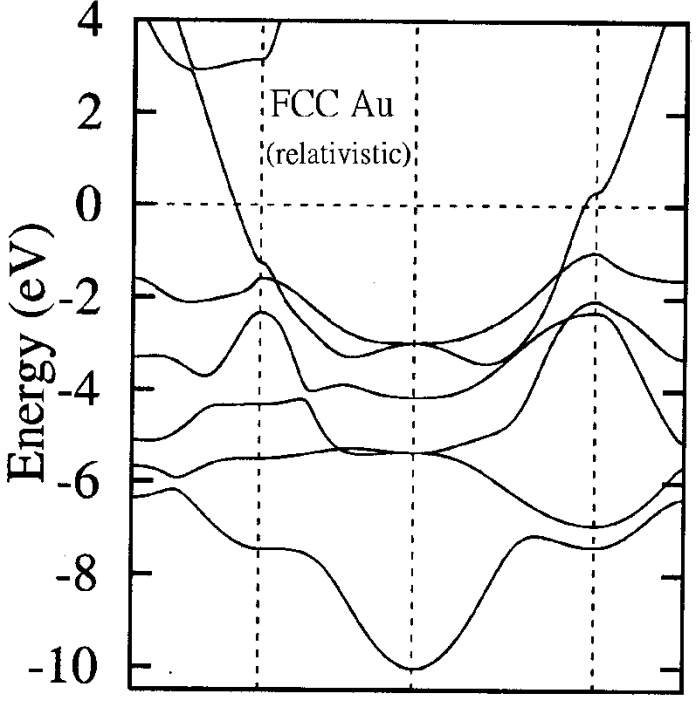

$$R = \frac{(\eta-1)^2+\kappa^2}{(\eta+1)^2+\kappa^2},$$

$$\kappa = \frac{1}{2}[(\varepsilon_1^2+\varepsilon_2^2)^{1/2}-\varepsilon_1^2]$$

$$\eta = \frac{1}{2}[(\varepsilon_1^2+\varepsilon_2^2)^{1/2}+\varepsilon_1^2].$$

$$\varepsilon_2 = \frac{4\pi^2}{\Omega\omega^2}\sum_{\mathbf{k},n,n'} |\left\langle \mathbf{k}n'\middle|\hat{p}_i\middle|\mathbf{k}n\right\rangle|^2 \times \delta(\varepsilon_{\mathbf{k}n'}-\varepsilon_{\mathbf{k}n}-\hbar\omega).$$

$$\varepsilon_1(\omega') = 1+\frac{2}{\pi}\int_0^\infty d\omega' \frac{\omega'\varepsilon_2(\omega')}{(\omega'^2-\omega^2)}.$$

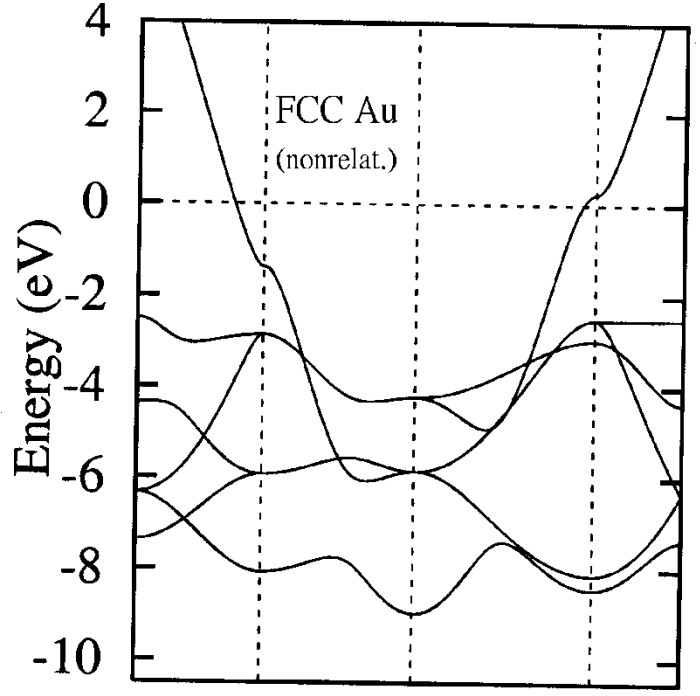

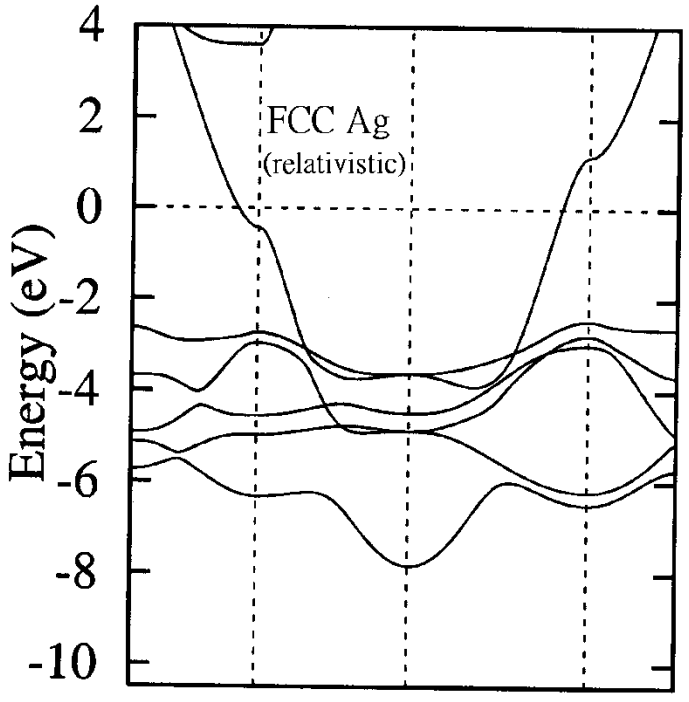

(b) Speakers, flash disc and magnetocrystalline anisotropy energy (MAE)

Ferromagnets (grains) need coercivity and hence MAE.

(relativistic) spin-orbit coupling

$$\frac{dV(r)}{dr}(\mathbf{s}\cdot\mathbf{L})$$

Magnetocrystalline anisotropy energy: total energy difference between two magnetization directions.

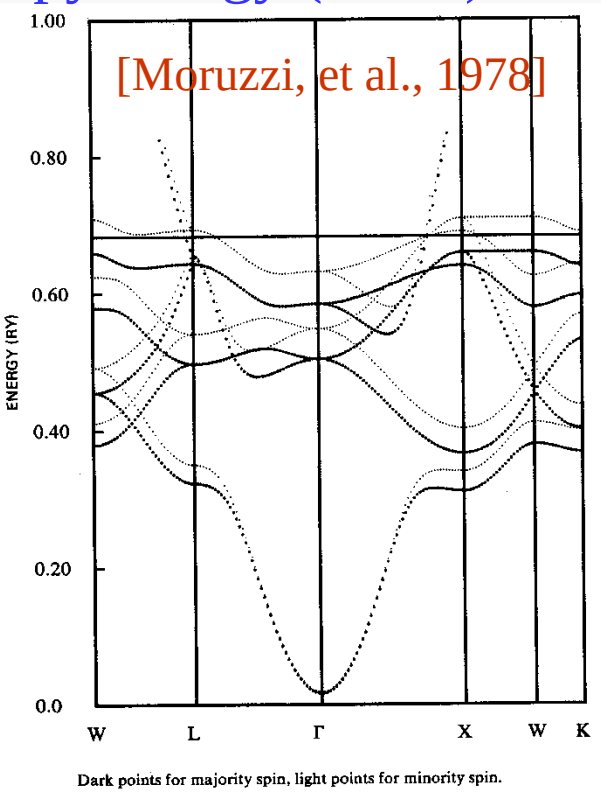

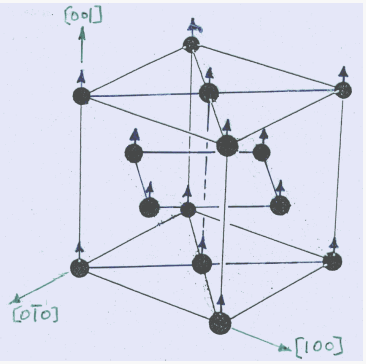

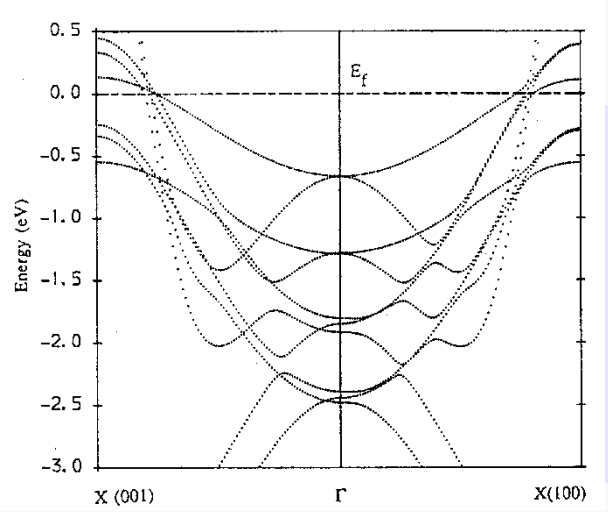

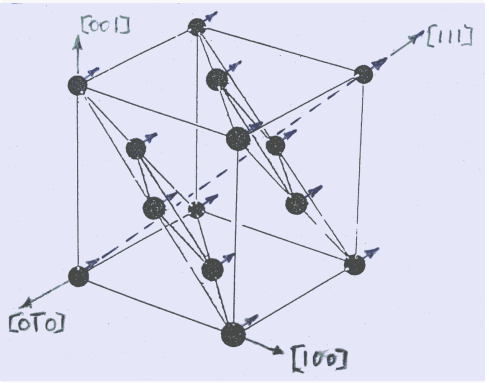

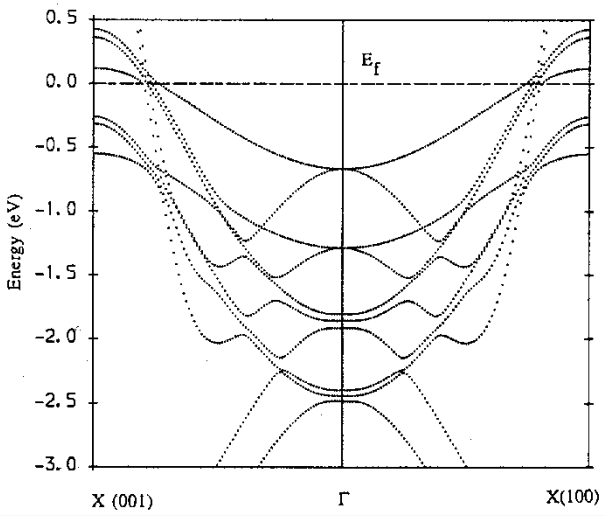

[Guo, et al., Physica B 172 (1991) 61]

Relativistic (spin-orbit coupling induced) effects in magnetic solids

Orbital magnetization;
X-ray circular dichroism;
Magneto-optical effects (Faraday rotation and Kerr effect);
Perpendicular magneto-crystalline anisotropy in multilayers;
Joule (anisotropic) magnetostriction;
Magneto-electric coupling;
… … .

Fundamental cause: the simultaneous occurrence of electron spin-polarization and relativistic interaction (spin-orbit coupling) in the magnetic solids (or the breaking of time-reversal symmetry).

(2) Relativistic spin-density functional theory

[e-e Breit interaction and diamagnetic effects neglected]

[Rajagopal, J. Phys. C 11 (1978) L943; MacDonald, Vosko, J. Phys. C 12 (1979) 2977]

Beginning with QED, following the same arguments as that of Hohenberg-Kohn-Sham, one ends up solving the effective 1-e Kohn-Sham-Dirac equ.

$$\{\frac{1}{i} c\alpha \cdot \nabla + (\beta - 1)c^2 + V_{eff,\sigma}(\mathbf{r}) + \beta\sigma \cdot \mathbf{B}_{eff}(\mathbf{r})\}\varphi_i(\mathbf{r}) = \varepsilon_i \varphi_i(\mathbf{r}) \qquad (9.4.1)$$

$$V_{eff}(\mathbf{r}) = V_{ext}(\mathbf{r}) + \int d\mathbf{r}' \frac{n(\mathbf{r}')}{|\mathbf{r}-\mathbf{r}'|} + \frac{\delta E_{xc}[n(\mathbf{r}), \mathbf{m}_s(\mathbf{r})]}{\delta n(\mathbf{r})}$$

$$\mathbf{B}_{eff}(\mathbf{r}) = V_{ext}(\mathbf{r}) + \frac{\delta E_{xc}[n(\mathbf{r}), \mathbf{m}_s(\mathbf{r})]}{\delta \mathbf{m}_s(\mathbf{r})}$$

$$n(\mathbf{r}) = \sum_i^N tr[\varphi_i^\dagger(\mathbf{r})\varphi_i(\mathbf{r})],$$

$$\mathbf{m}_s(\mathbf{r}) = \sum_i^N tr[\varphi_i^\dagger(\mathbf{r})\beta\sigma_z\varphi_i(\mathbf{r})],$$

$$\mathbf{m}_o(\mathbf{r}) = \sum_i^N tr[\varphi_i^\dagger(\mathbf{r})\beta l_z\varphi_i(\mathbf{r})].$$

(3) Orbital magnetization (moment)

Formation of orbital magnetic moment

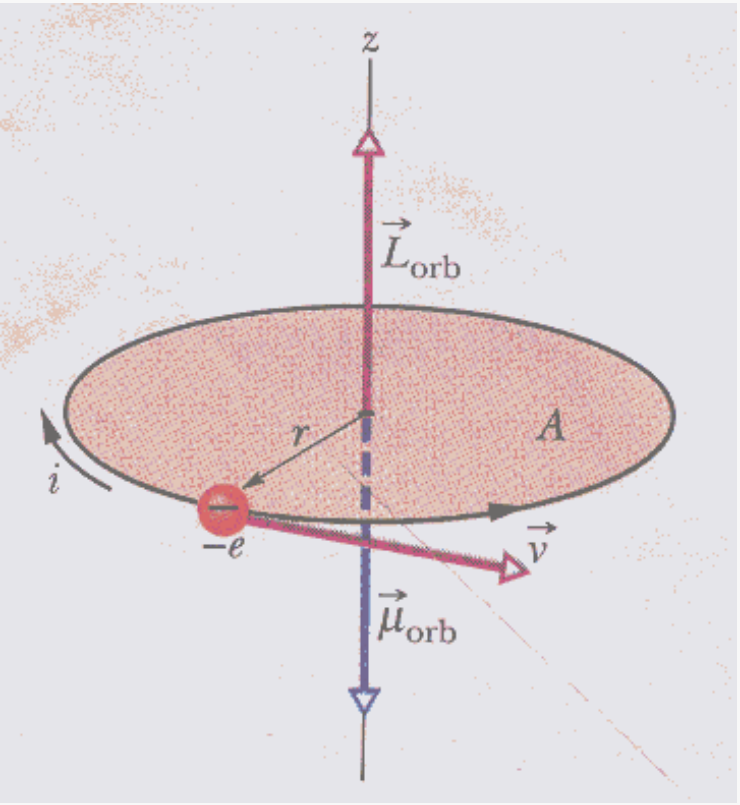

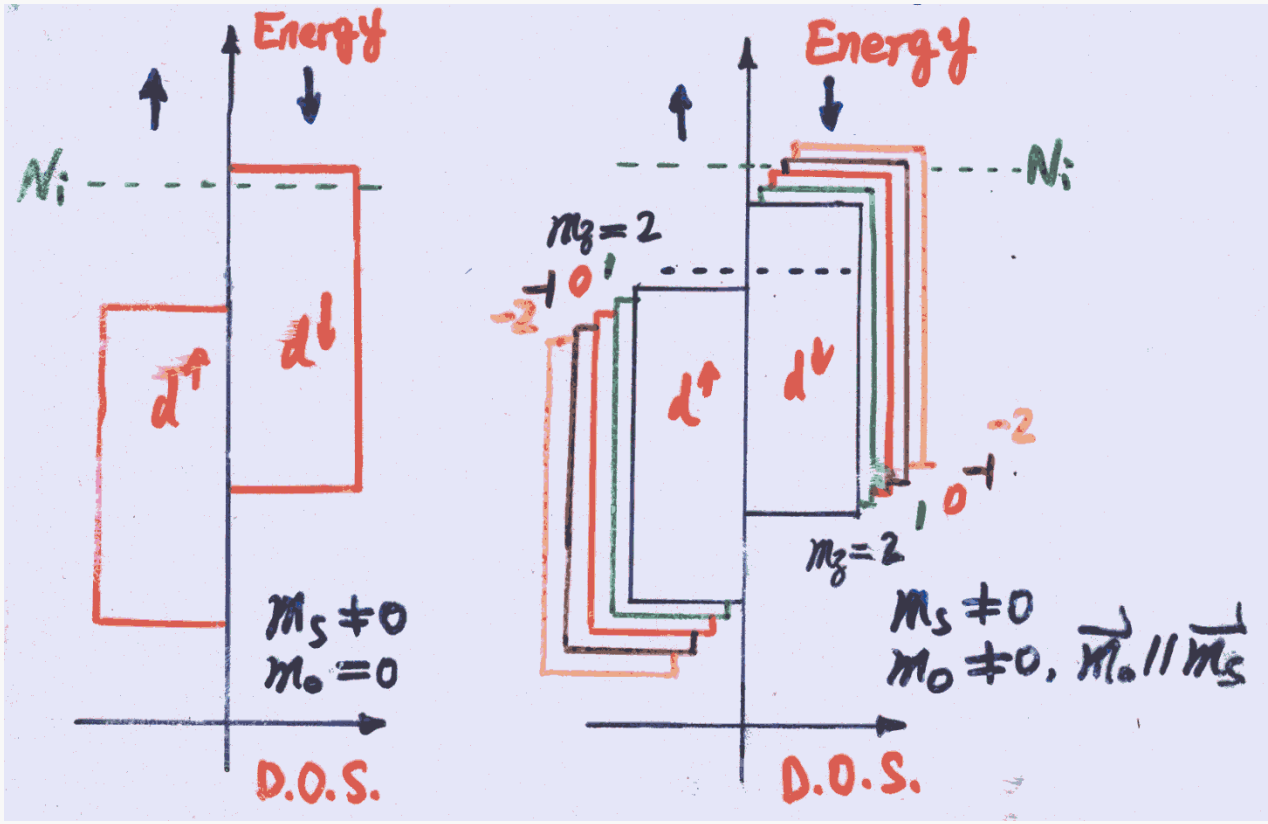

(4) Magnetic circular dichroism in x-ray absorption

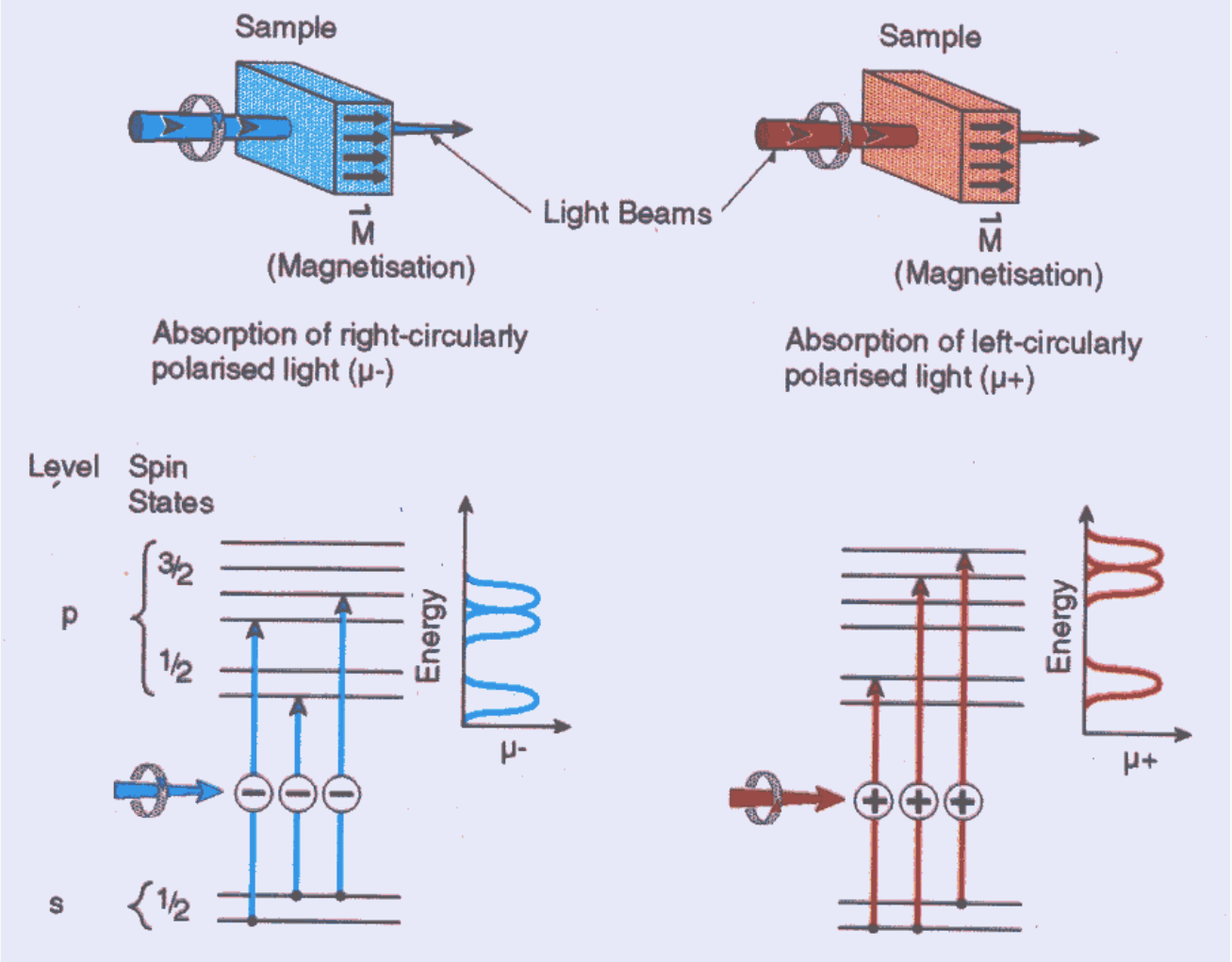

Origin of magnetic circular dichroism (MCD)

(a) Magnetization but no SOC:
No MCD

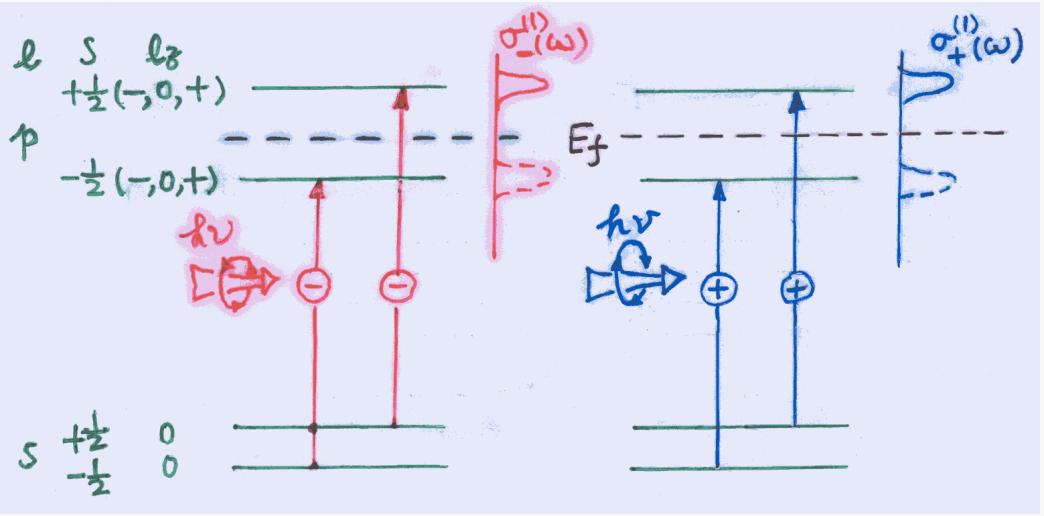

(b) No magnetization but SOC on:
No MCD

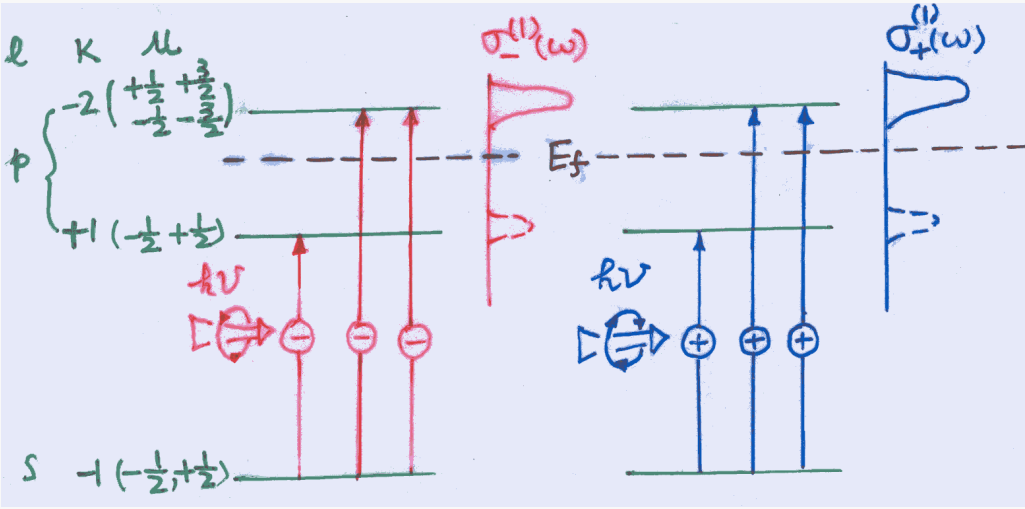

(c) Magnetization and SOC:
Yes, MCD

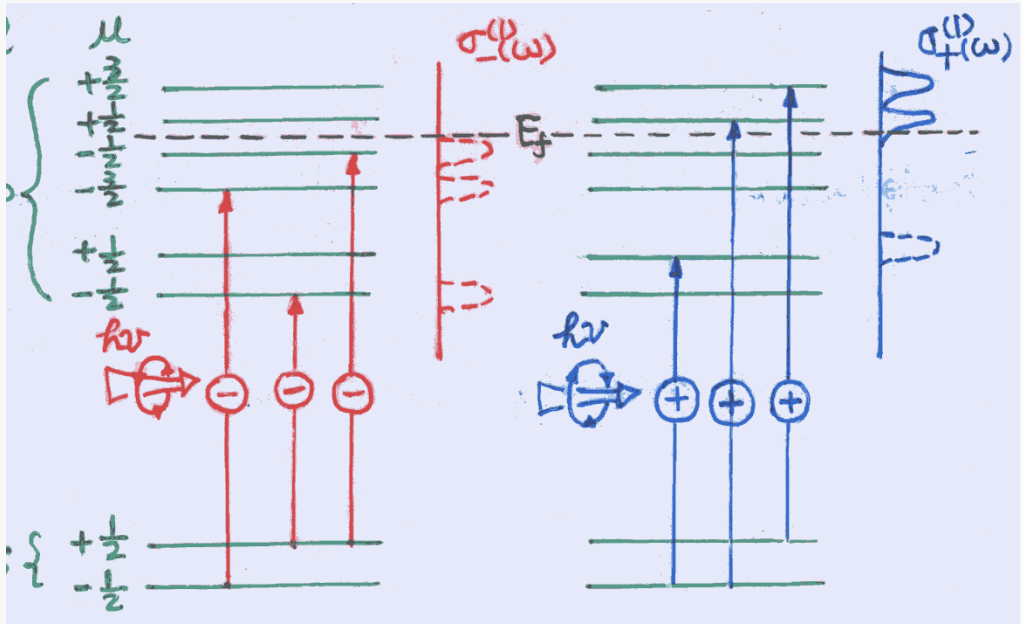

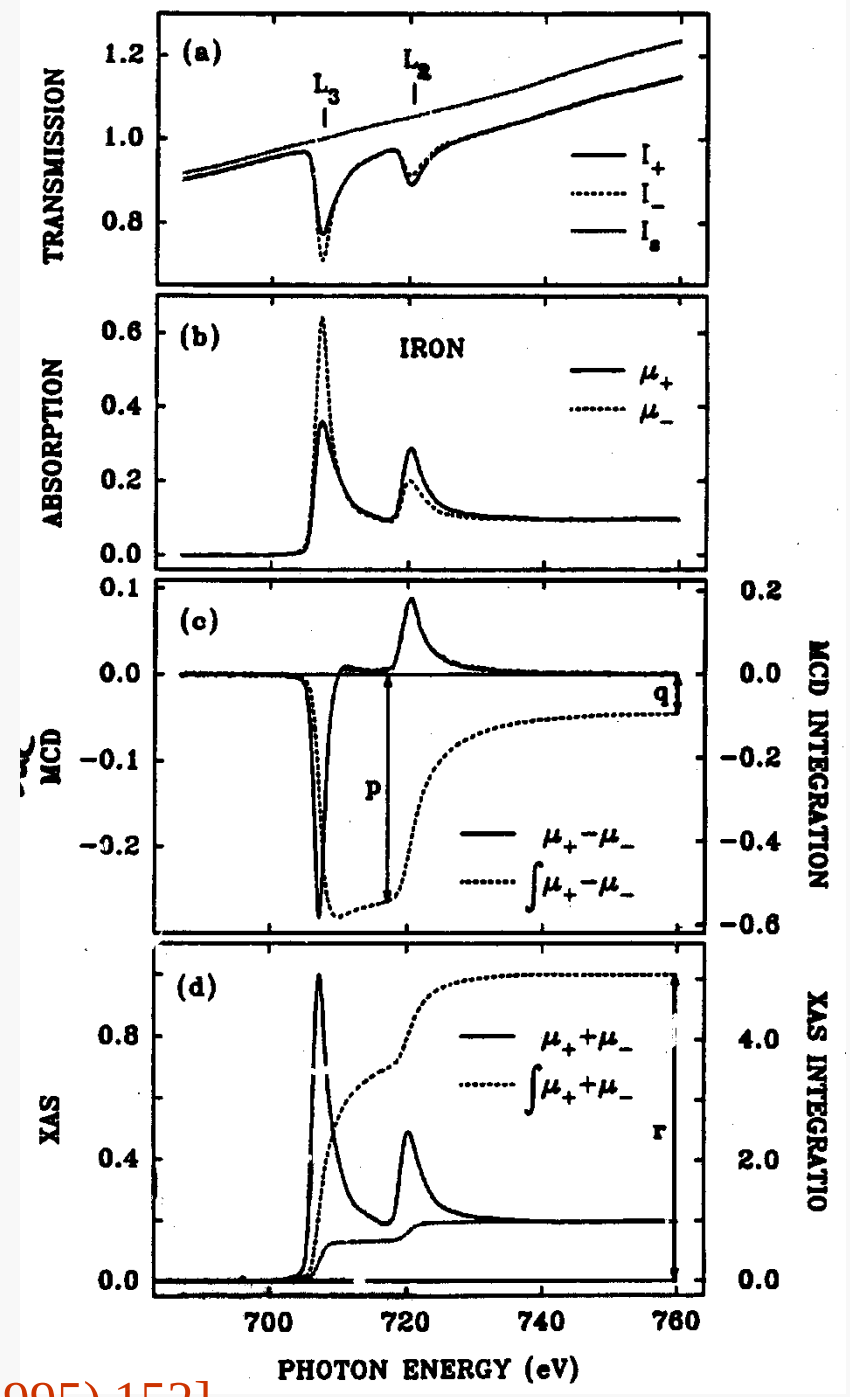

[Chen, et al., PRL 75 (1995) 152]

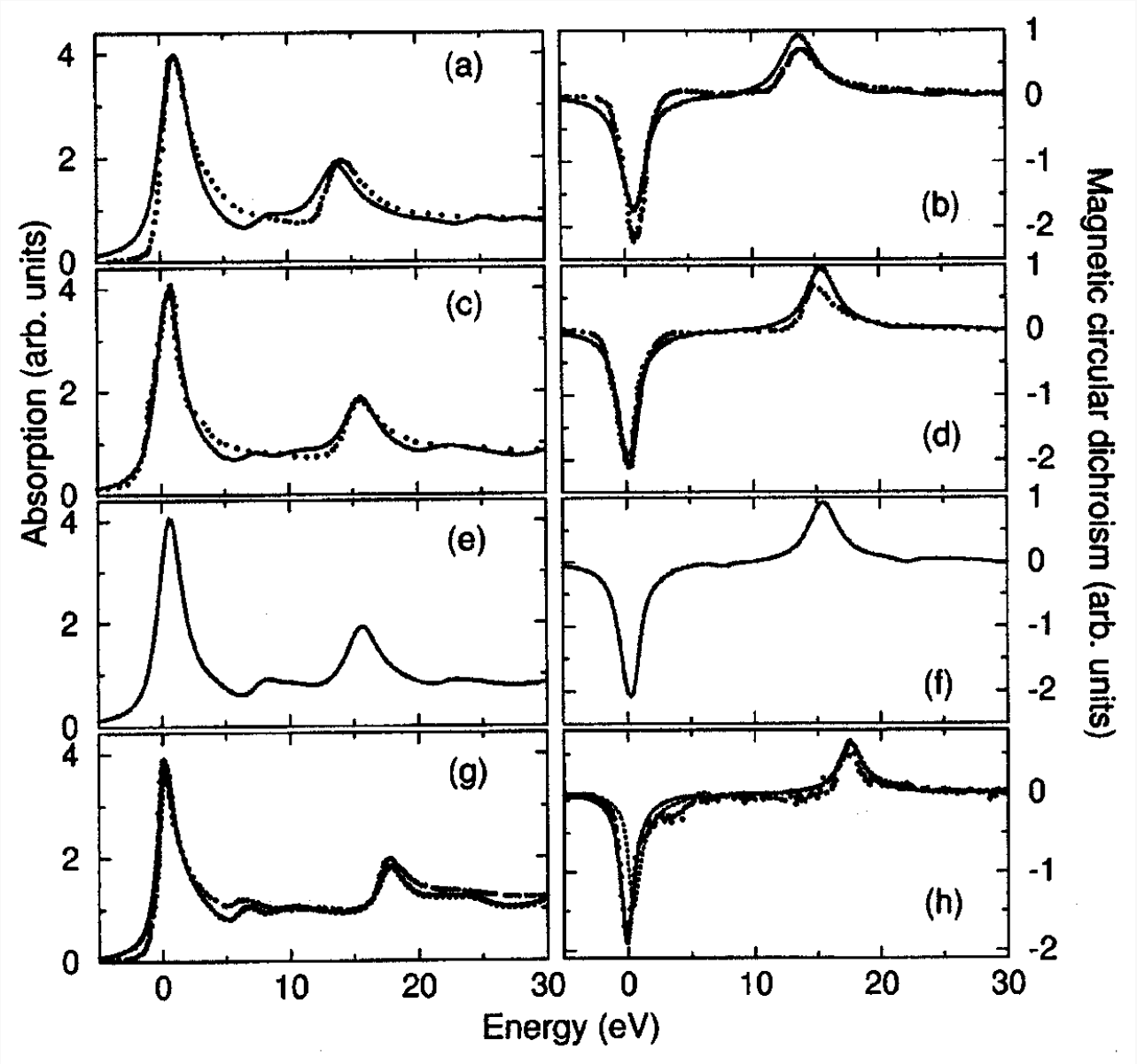

[Guo, PRB 55 (1997) 11619]

(5) Magneto-optical properties

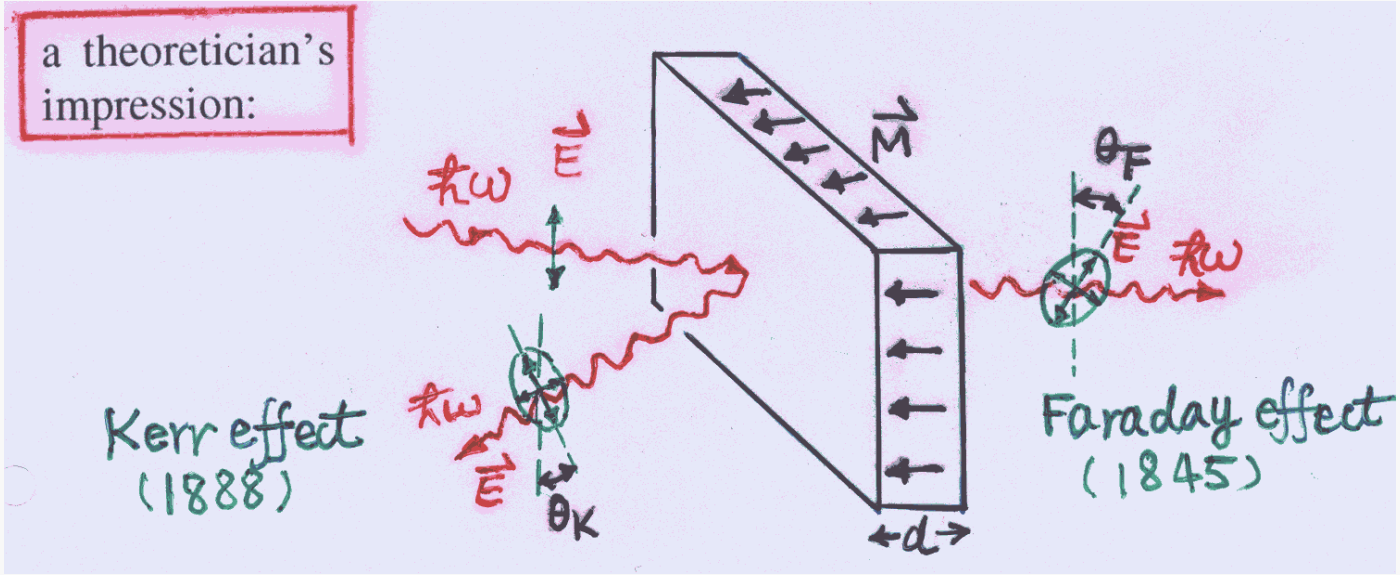

Macroscopic theory

For solids with at least orthorhombic symmetry,

$$\sigma(\omega) = \begin{bmatrix} \sigma_{xx} & \sigma_{xy} & 0 \\ -\sigma_{xy} & \sigma_{yy} & 0 \\ 0 & 0 & \sigma_{zz} \end{bmatrix} = \sigma_1(\omega) + i\sigma_2(\omega) \qquad (9.4.2)$$

$$\sigma_{xx} \approx \sigma_{yy} \approx \frac{1}{2}(\sigma_+ + \sigma_-), \sigma_{xy} = \frac{1}{2}(\sigma_+ - \sigma_-); \varepsilon_{ij} = \delta_{ij} + i\frac{4\pi}{\omega}\sigma_{ij}. \qquad (9.4.3)$$

Faraday rotation

$$\theta_F(\omega) = \frac{\omega d}{2c}\,\mathrm{Re}[n_+ - n_-],\ n_\pm = \sqrt{1 + i\frac{4\pi}{\omega}\sigma_\pm}. \qquad (9.4.4)$$

Kerr effect

$$\theta_K(\omega) = \mathrm{Re}[\frac{\sigma_{xy}}{i\sigma_{xx}n}] = \mathrm{Re}[\frac{1/2(\sigma_+ - \sigma_-)}{i(\varepsilon_{xx} - 1)\sqrt{\varepsilon_{xx}}}],\ \varepsilon_K(\omega) = \mathrm{Im}[\frac{\sigma_{xy}}{i\sigma_{xx}n}]. \qquad (9.4.5)$$

Thus, the origin of Faraday and Kerr effects are also magnetic circular dichroism, i.e., in the optical photon energy range.

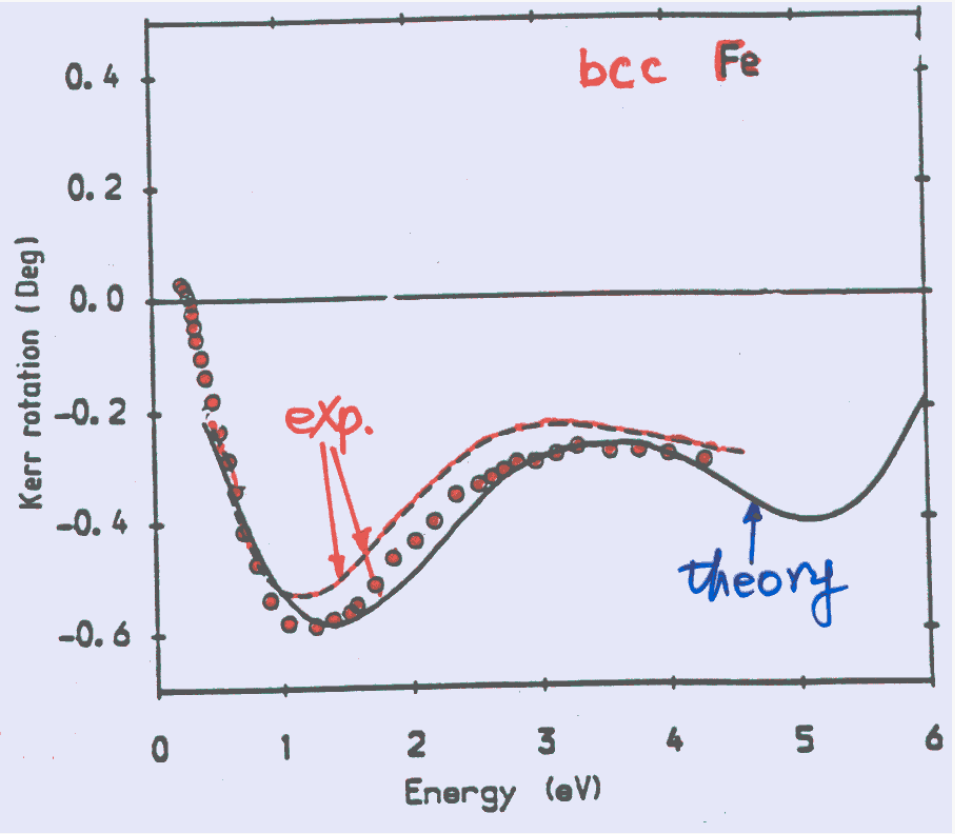

[Guo, Ebert, PRB 51 (1995) 12633]

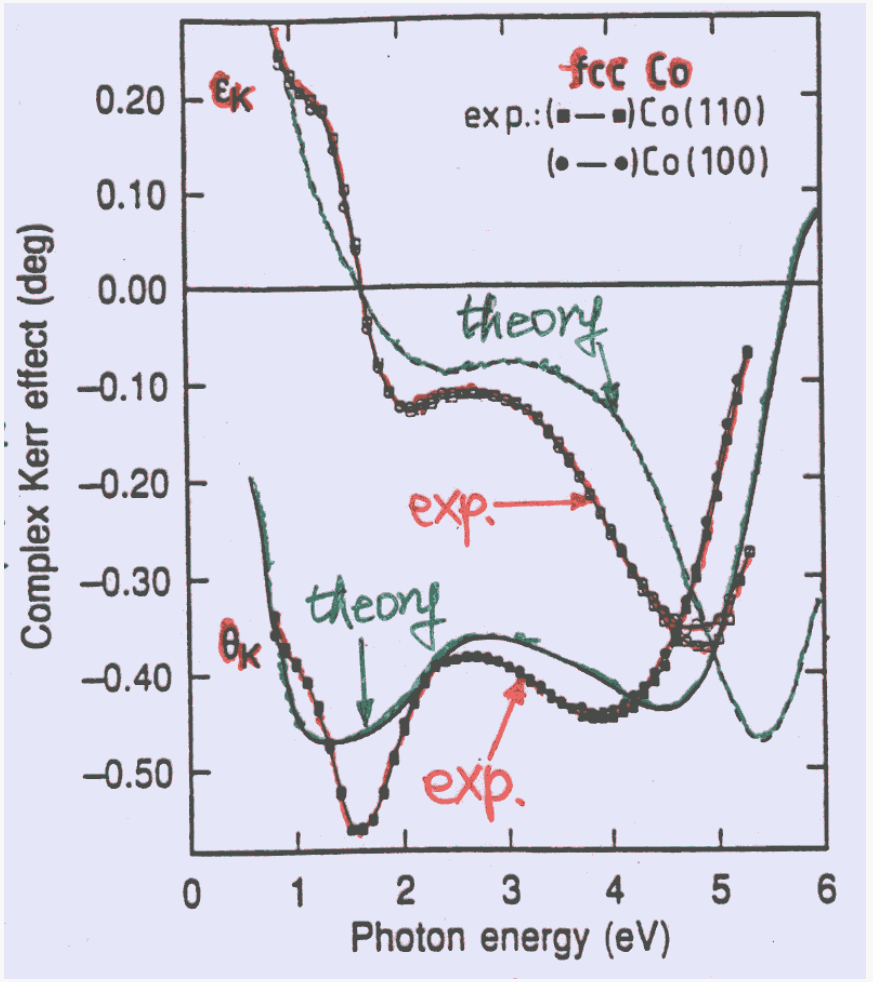

[Guo, Ebert, PRB 50, 1994]

(5) Magneto-crystalline anisotropy energy (Joule magnetostriction)

Definition

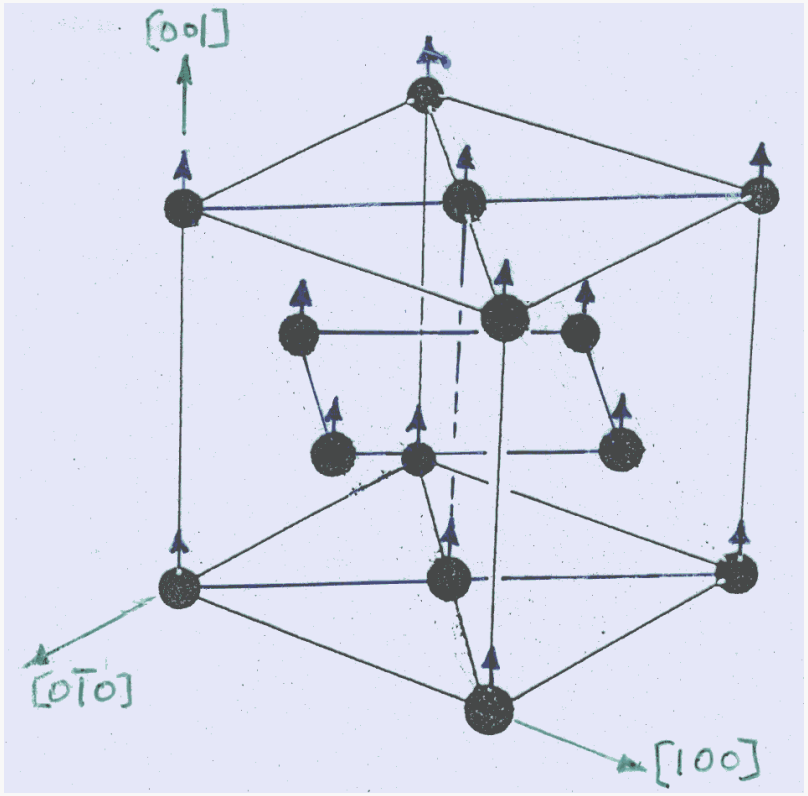

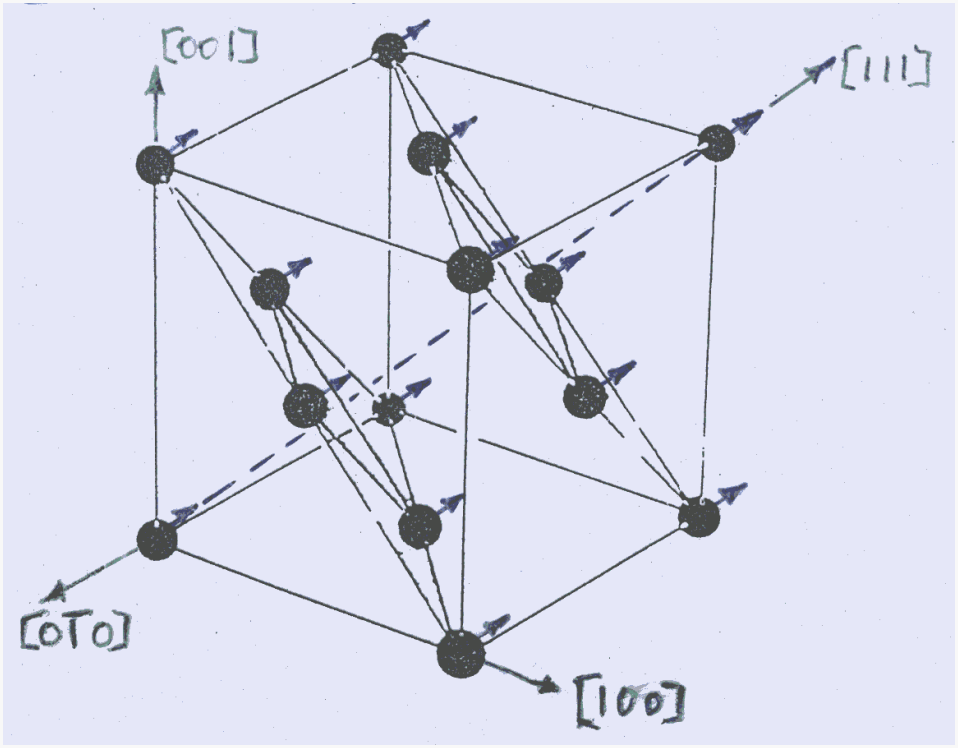

Origin of the magneto-crystalline anisotropy energy

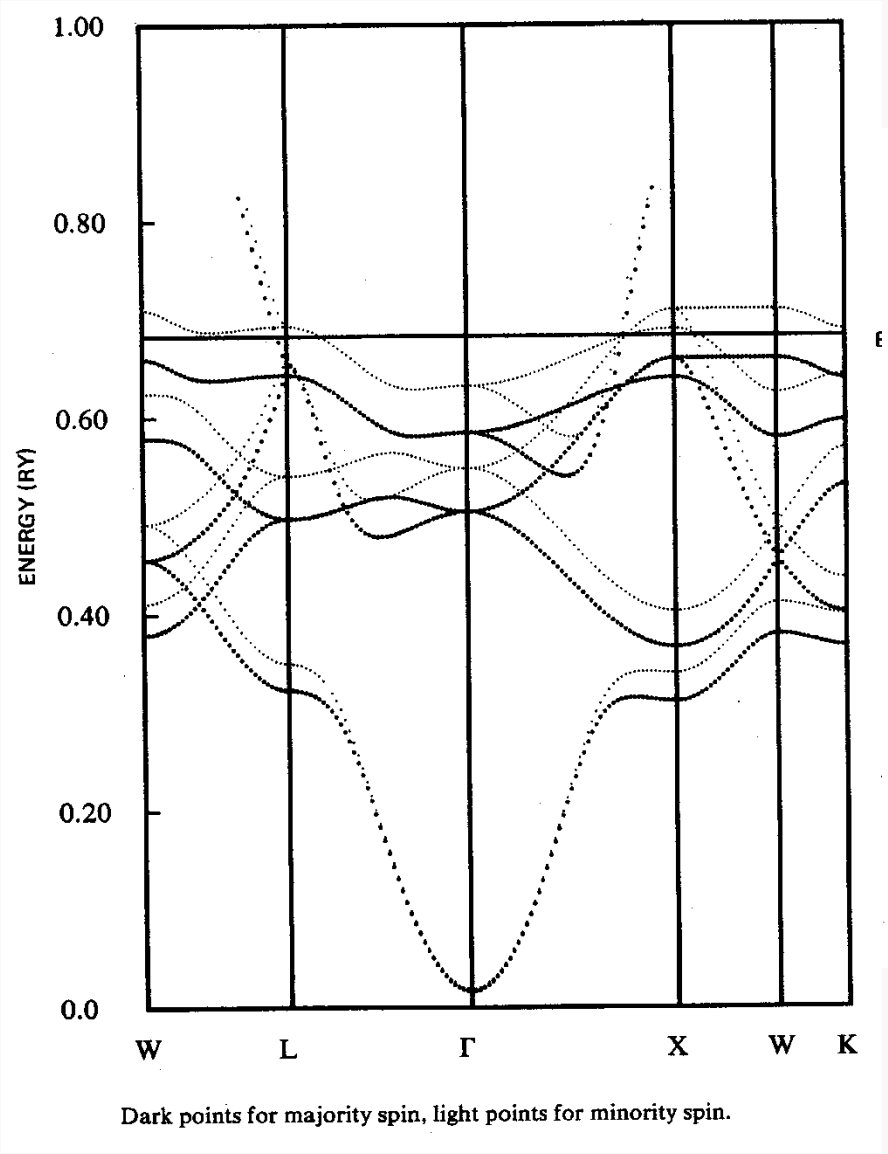

Dark points for majority spin, light points for minority spin.

[Moruzzi, et al., 1978]

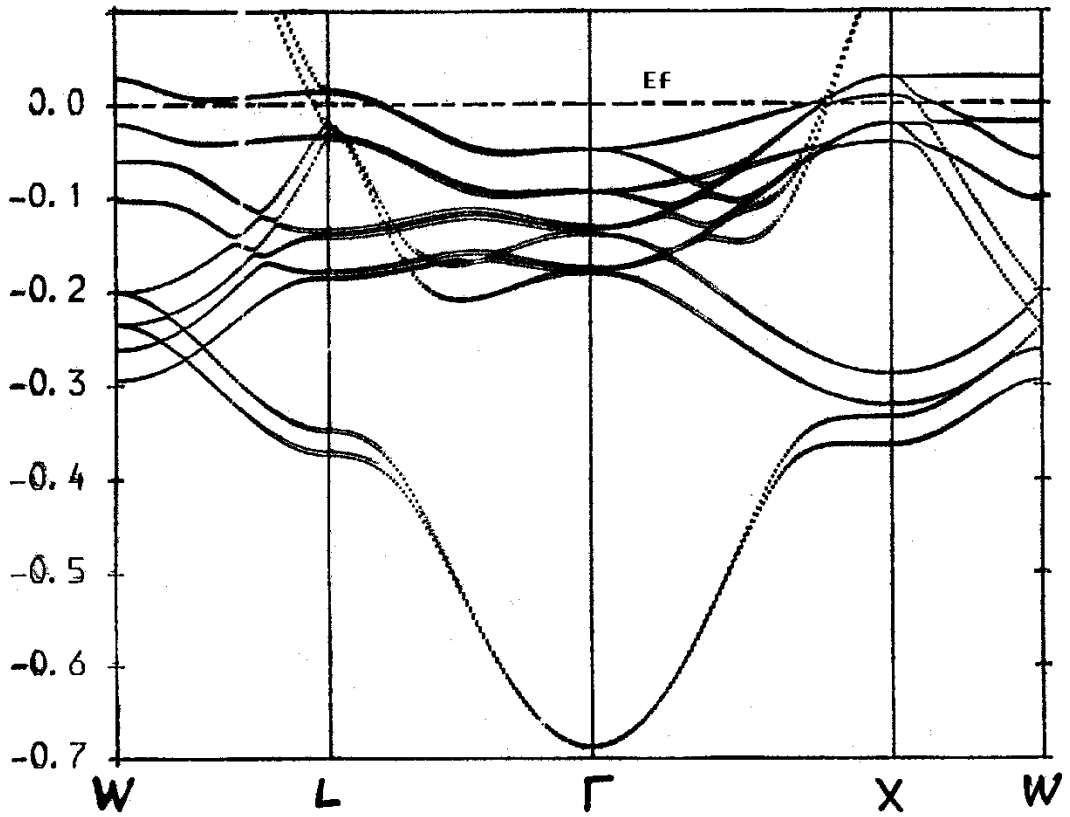

[Guo, et al., Physica B 172 (1991) 61]

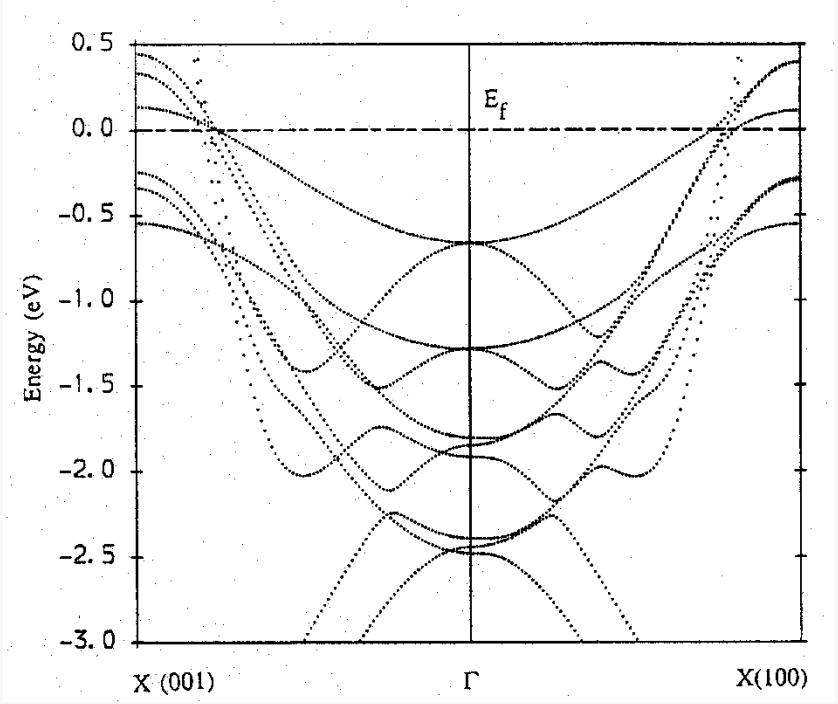

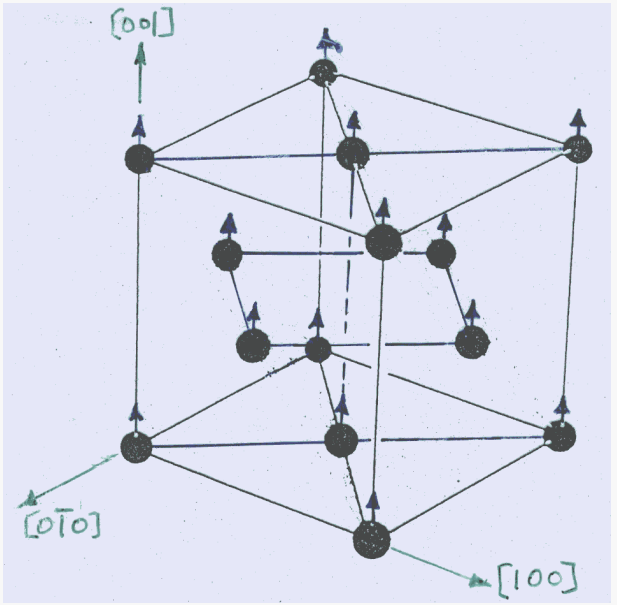

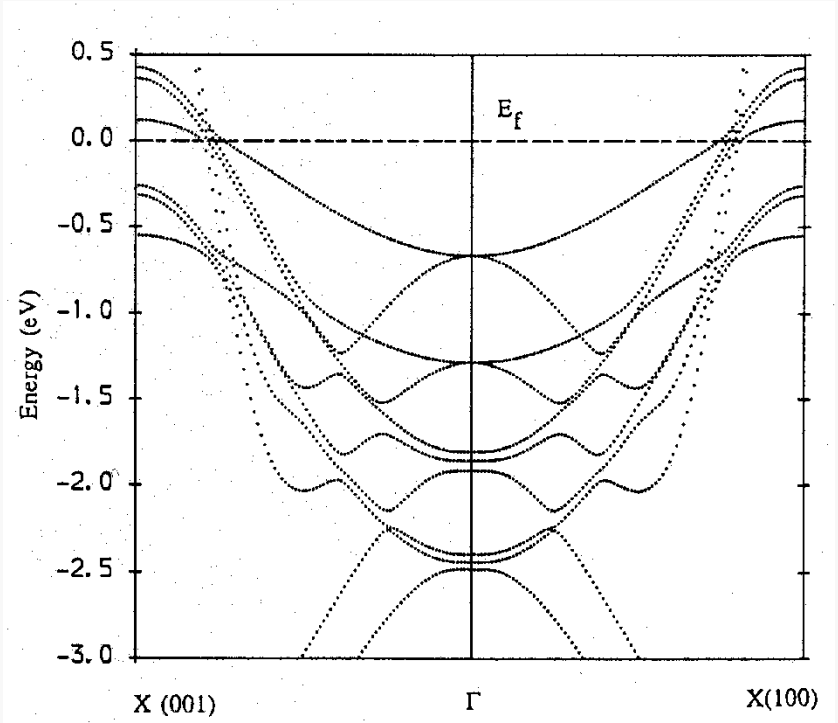

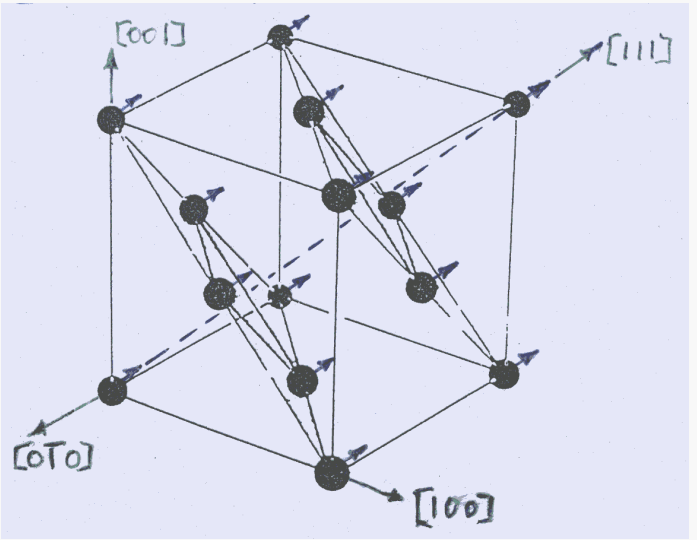

[Guo, et al., Physica B 172 (1991) 61]

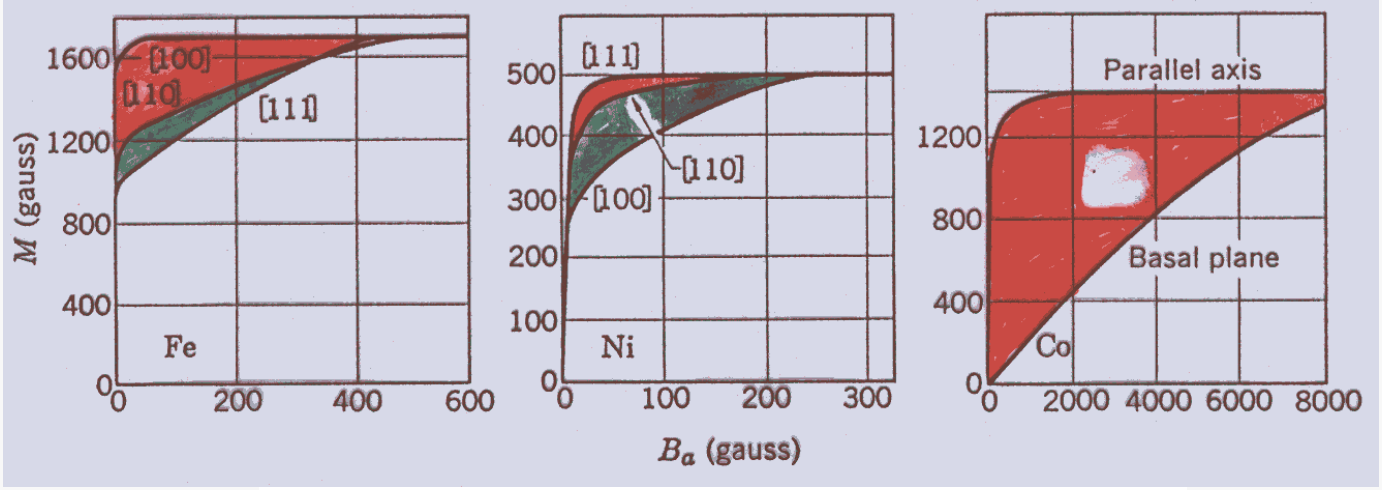

[Kittel]

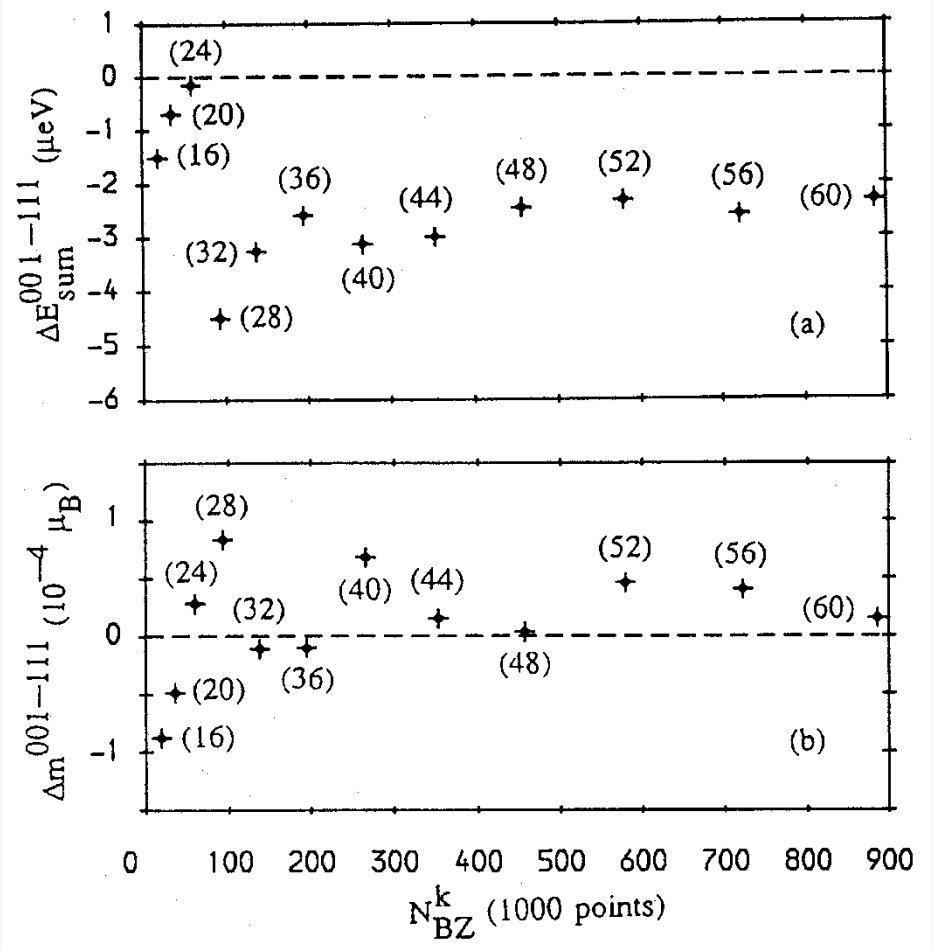

[Guo, et al., Physica B 172 (1991) 61]

9.5. Magnetism on surfaces and in thin films

(1) Interesting magnetic properties of surfaces and thin films

(i) 2D (surface/interface) magnetism
enhanced magnetization; making nonmagnetic metals magnetic
(ii) Effects of dimensionality cross-over
(iii) Perpendicular magnetic anisotropy
(iv) Enhanced magneto-optical properties
… … .

(2) Surface and thin films electronic structure calculations

(a) A slab-supercell approach to the surface and thin film problem

A slab-supercell geometry for a surface of a bulk solid.

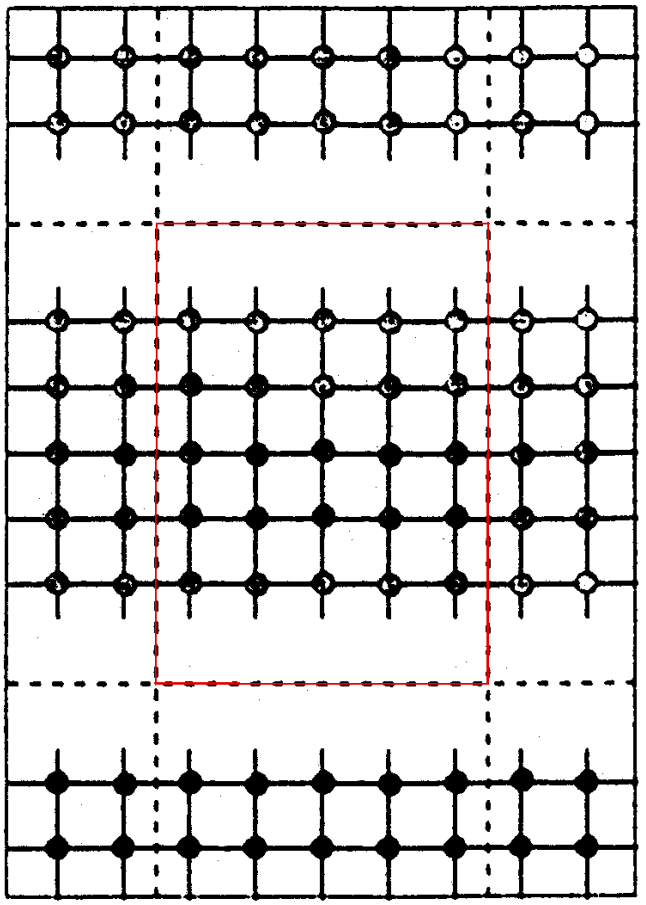

Disadvantages:

(i) A thick vacuum layer may be needed, which neccessitate a large number of basis functions;

(ii) For a surface, a thick slab may also be needed to avoid the surface-surface interaction (e.g., GaAs (110), > 11 ML; for a metal surface, 7 ML) .

(b) Thin film approach, e.g., Film FLAPW method

(*Jepsen, et al., PRB 18 ('78) 605; Krakauer, et al., PRB 19 ('79) 1706*)

space divided into three regions:

I: muffin-tin spheres;

II: interstitial region;

III: vacuum region.

The LAPW basis functions

$\{\mathbf{G}_m\}$: 2-D reciprocal lattice;

$\mathbf{k}$: 2-D $\mathbf{k}$-space vector.

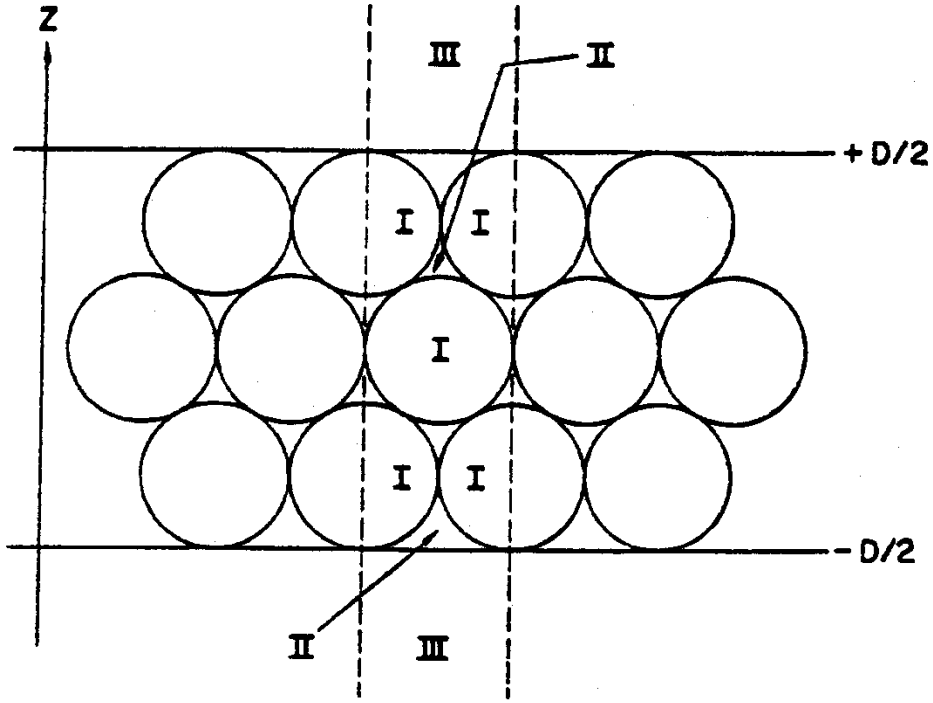

FIG. 1. Schematic representation of the film-muffin-tin (FMT) potential for a three-layer film. The unit cell, indicated by dashed lines, extends to $z = \pm\infty$. There are two boundary planes at $z = \pm \frac{1}{2}D$.

$$\sum_L [A_L^{mn} u_l(|\mathbf{r} - \boldsymbol{\tau}_i|, \varepsilon_{vl}) + B_L^{mn} \dot{u}_l(|\mathbf{r} - \boldsymbol{\tau}_i|, \varepsilon_{vl})] Y_L(\mathbf{r} - \boldsymbol{\tau}_i), (L \equiv lm) \quad \text{(I)}$$

$$\phi_{mn}(\mathbf{k}, \mathbf{r}) = \begin{cases} \Omega^{-1/2} e^{i(\mathbf{k}+\mathbf{G}_m)\cdot\mathbf{r}} e^{ik_n z}, & (k_n \equiv \frac{n2\pi}{D}, n = 0,1,2,\ldots; \frac{1}{2}, \frac{3}{2}, \frac{5}{2}, \ldots) \quad \text{(II)} \\ [C_{mn}^{(i)} u_{\mathbf{k}m}(z, \varepsilon_v) + D_{mn}^{(i)} \dot{u}_{\mathbf{k}m}(z, \varepsilon_v)] e^{i(\mathbf{k}+\mathbf{G}_m)\cdot\mathbf{r}}, i = 1,2. & \quad \text{(III)} \end{cases}$$

where $u_{\mathbf{k},m}(z,\varepsilon_\nu)$ is a solution of the 1-D Schroedinger equ. in region III with z-dependent potential, *V(z)*,

$$\left\{-\frac{d^2}{dz^2}+V(z)-[\varepsilon_\nu-(\mathbf{k}+\mathbf{G}_m)^2]\right\}u_{\mathbf{k},m}(z,\varepsilon_\nu)=0.$$

The coefficients C_{mn} and D_{mn} are determined by matching the basis functions and their derivatives across the boundary planes at $z=\pm\frac{1}{2}D$.

Advantages: the size of the eigenvalue problem is determined only by the size of the surface unit cell and the slab thickness *D*.

(3) Enhanced magnetization

system		m_s (μ_B)	m_o (μ_B)
Bulk bcc Fe		2.108	0.044
Fe (001) Surface	Fe1 Fe2	3.032 2.212	0.087 0.046
1 Fe monolayer on Cu (001)	Fe Cu	2.73 0.02	
Fe bilayer on Pd (001)	Fe1 Fe2 Pd	2.894 2.881 0.236	
Ag/Fe(1 ML)/Ag (001)	Fe Ag	2.952 -0.025	0.118 0.002
Au/Fe(1 ML)/Au (001)	Fe Au	3.046 0.001	0.094 0.015
1 Ru monolayer on Ag (001)	Ru	1.73	

(4) Making nonmagnetic metals magnetic

Only 5 non-*f* metals are magnetic:

Ferromagnets
Fe: 2.2 μ_B
Co: 1.6 μ_B
Ni: 0.6 μ_B

Antiferromagnets
Cr: 0.6 μ_B
Mn: 2.3 μ_B

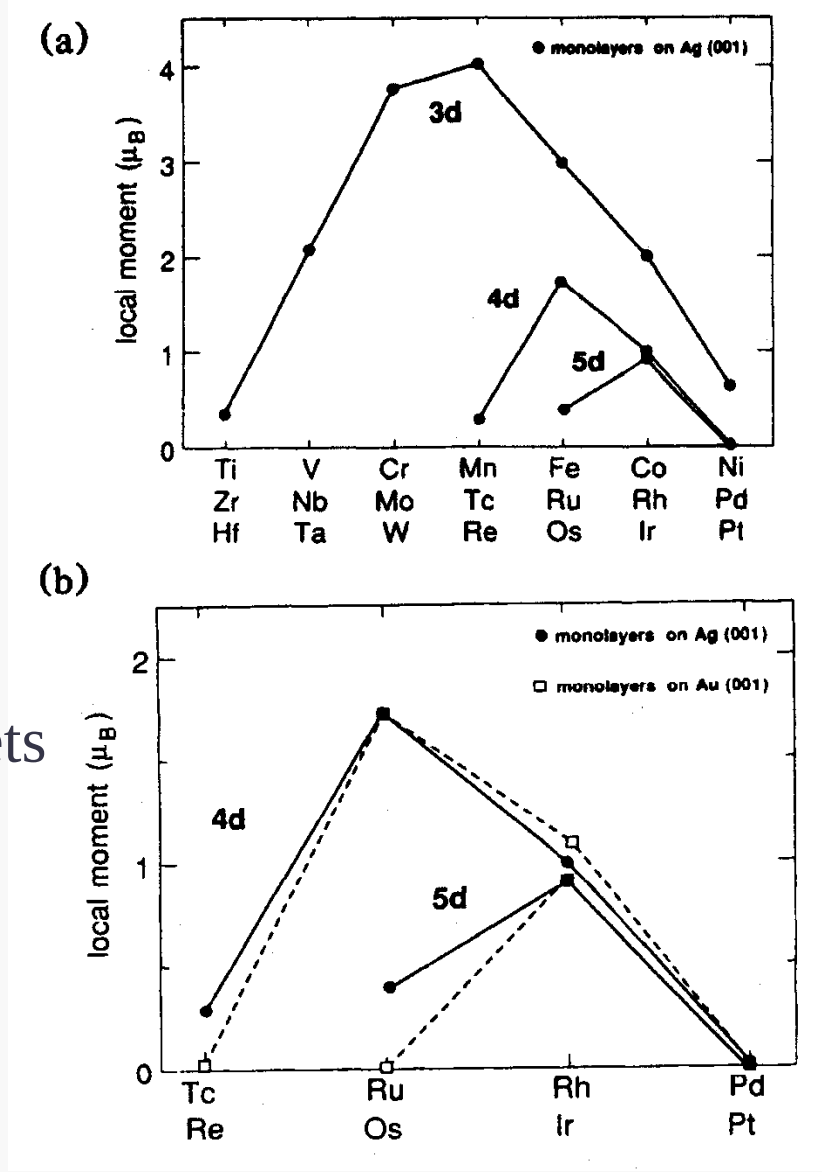

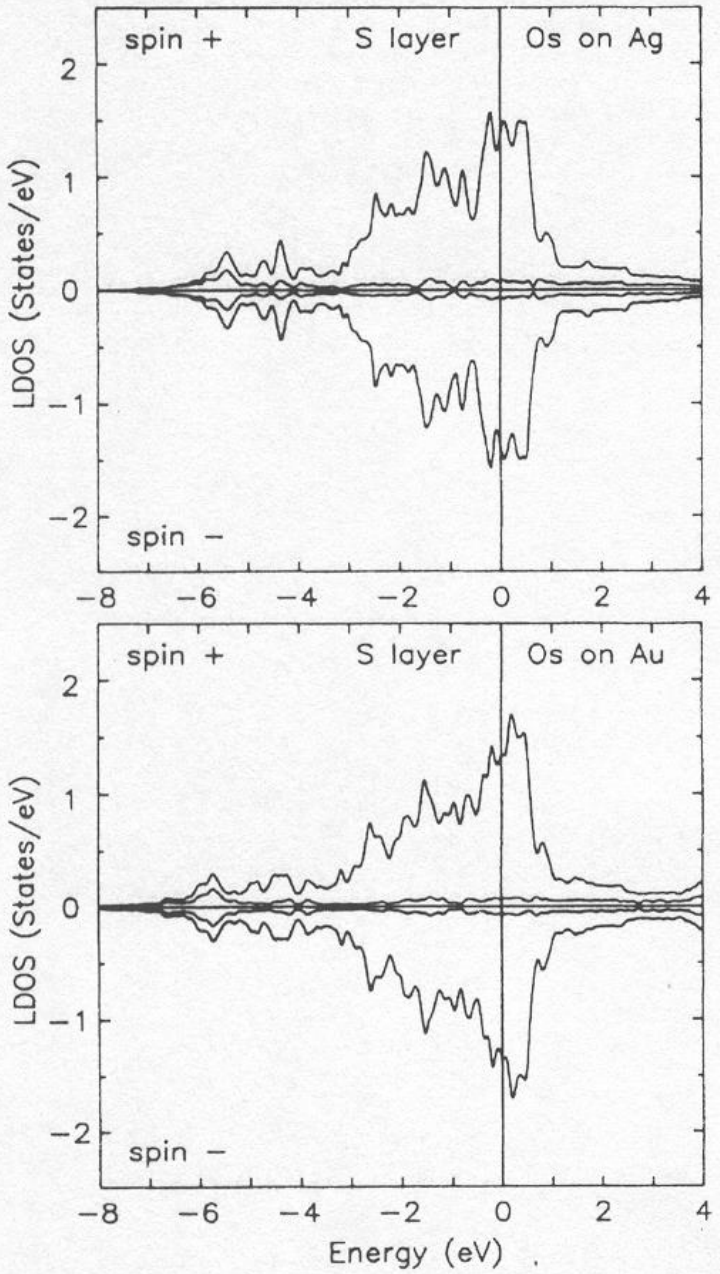

[Blugel, PRL 68 (1992) 851]

(5) Dimensionality cross-over

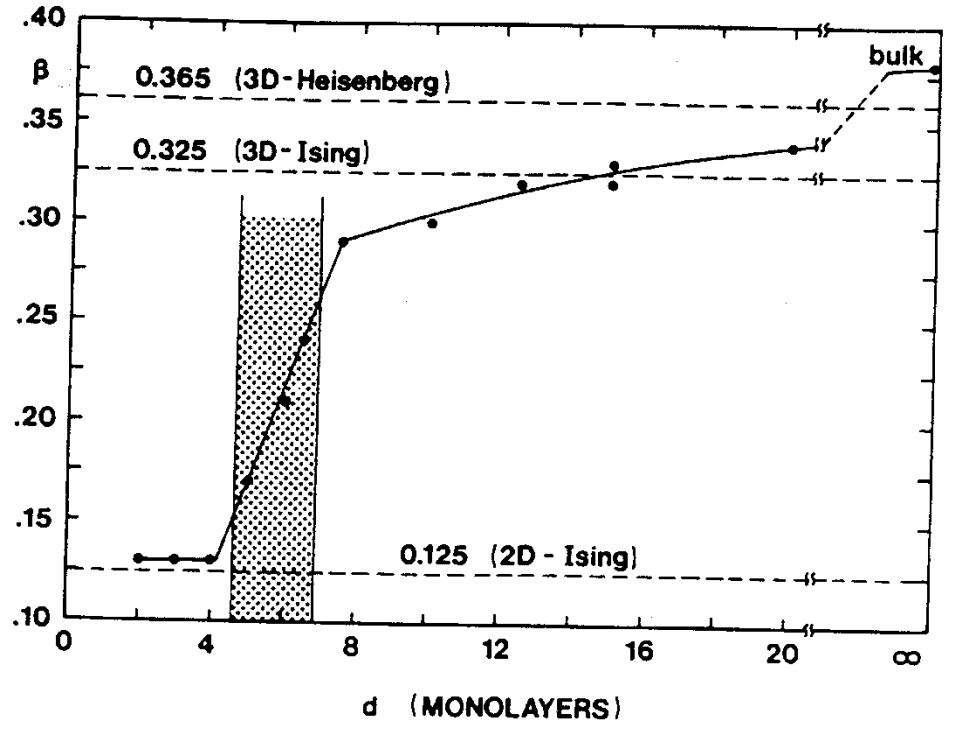

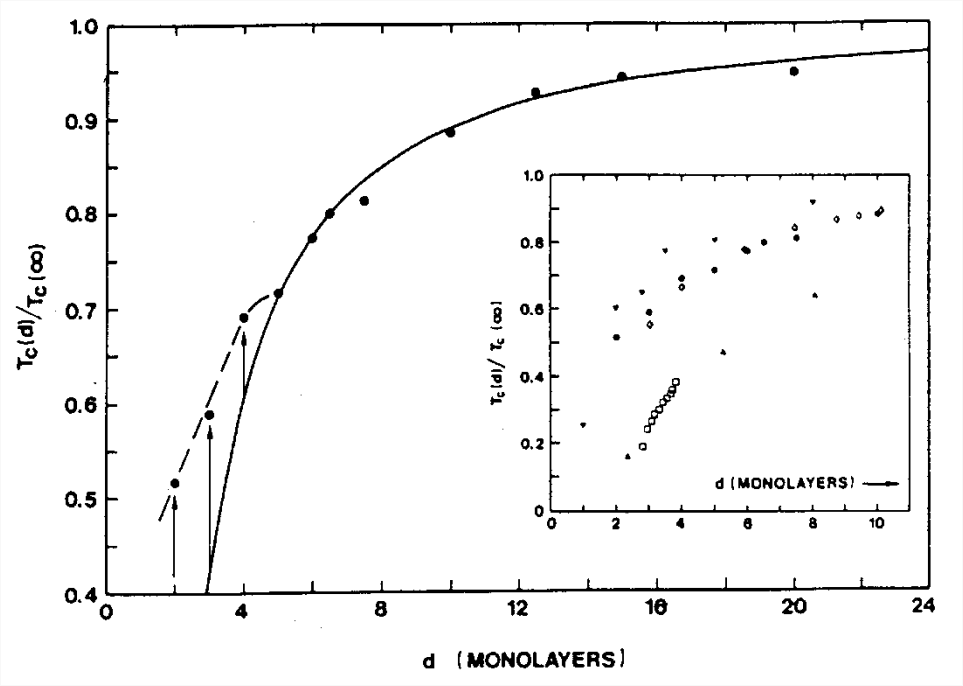

[Li, Baberschke, PRL 68 (1992) 120]

(6) Magnetocrystalline anisotropy energy

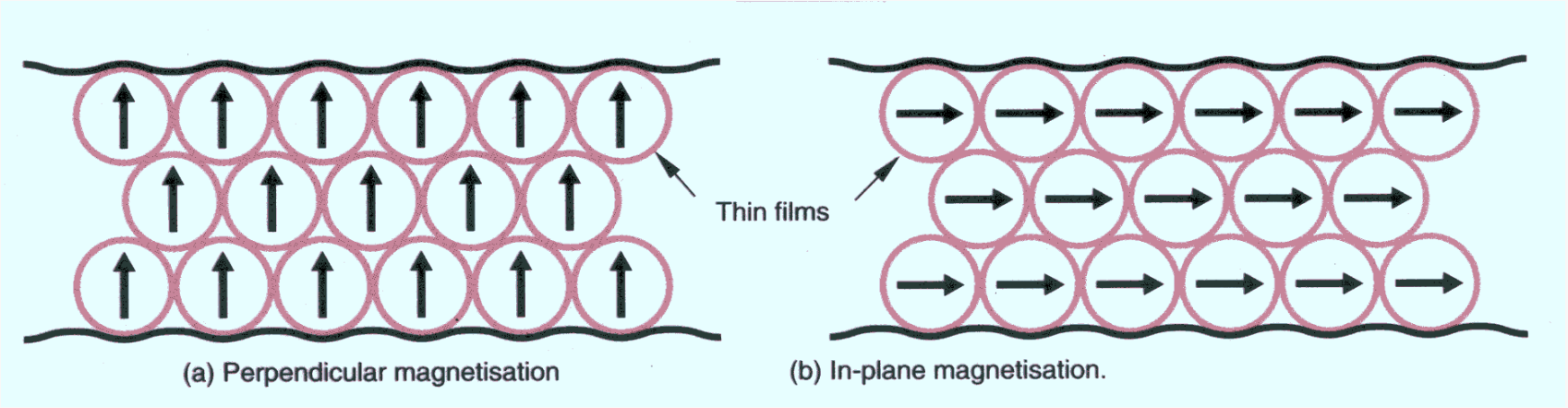

Origins and size of perpendicular magnetic anisotropy energy?

Model Hamiltonian for a 2D spin lattice

$$H = H_{ex} \quad \text{(Heisenberg model)}$$

$$+ H_{dip} \quad \text{(dipole-dipole interaction)}$$

$$+ H_{so} \quad \text{(anisotropic interaction)}$$

$$H = -\frac{1}{2} J \sum_{<ij>} \mathbf{m}_i \cdot \mathbf{m}_j$$

$$+ \frac{1}{2} \omega \sum_{ij} \left[\frac{(\mathbf{m}_i \cdot \mathbf{m}_j)}{r_{ij}^3} - 3 \frac{(\mathbf{m}_i \cdot \mathbf{r}_{ij})(\mathbf{m}_j \cdot \mathbf{r}_{ij})}{r_{ij}^5} \right]$$

$$\lambda \sum_i (m_i^z)^2$$

Applications:

Two essential properties of a magnetic thin films for high density magnetic-optic recording:

(a) Large Kerr effect at small laser wavelength (e.g., green or blue);

(b) Large perpendicular magnetic anisotropy (PMA).

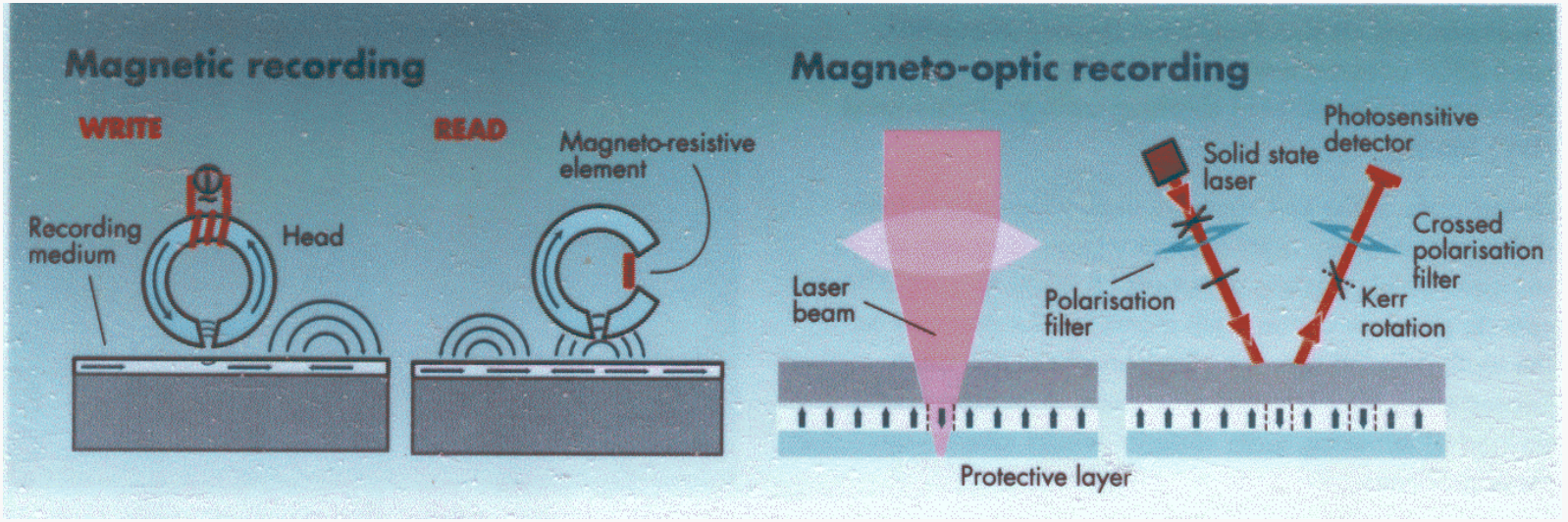

Calculated anisotropy energies

Fe monolayers

	ΔE_e^{z-x} (meV/Fe)	ΔE_d^{z-x} (meV/Fe)	ΔE_t^{z-x} (meV/Fe)	ΔE_{exp}^{z-x} (meV/Fe)	
Free Fe ML	+0.010	+0.205	+0.215		
Cu/Fe/Cu	-0.417	+0.136	-0.281		
Ag/Fe/Ag	-0.796	+0.143	-0.653		
Au/Fe/Au	-0.743	+0.149	-0.594		

[Guo, et al., JPCM 3 (1991) 8205]

Fe/Ag multilayers

	ΔE_e^{z-x} (meV/Fe)	ΔE_d^{z-x} (meV/Fe)	ΔE_t^{z-x} (meV/Fe)	ΔE_{exp}^{z-x} (meV/Fe)	
Fe_1Ag_5	-0.796	+0.112	-0.684		
Fe_3Ag_5	-0.588	+0.239	-0.349		
Fe_5Ag_3	-0.217	+0.302	-0.085		

[Guo, et al., JMMM 104-107 (1992) 1772]

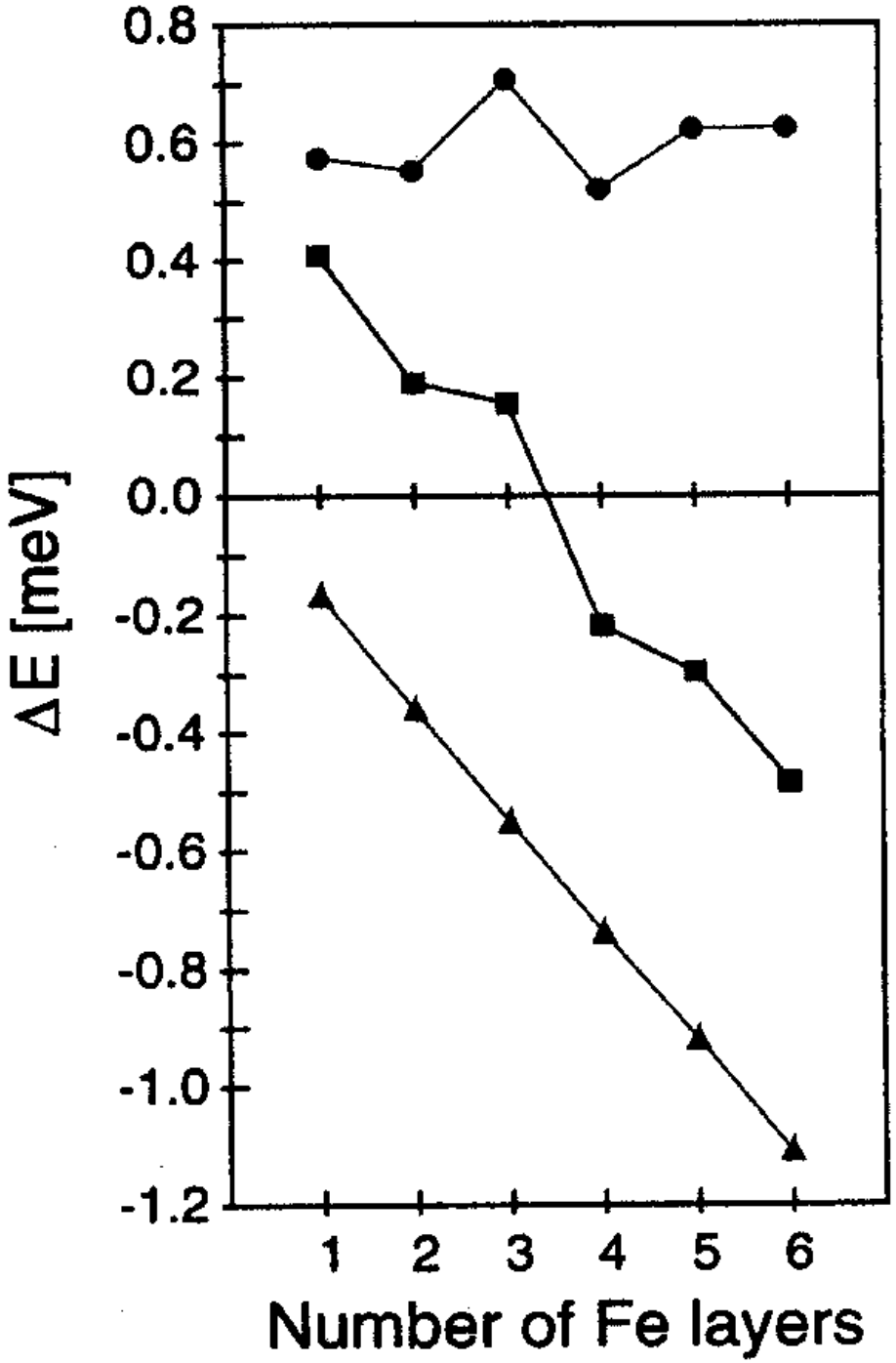

[Szunyogh, et al., PRB 1995]

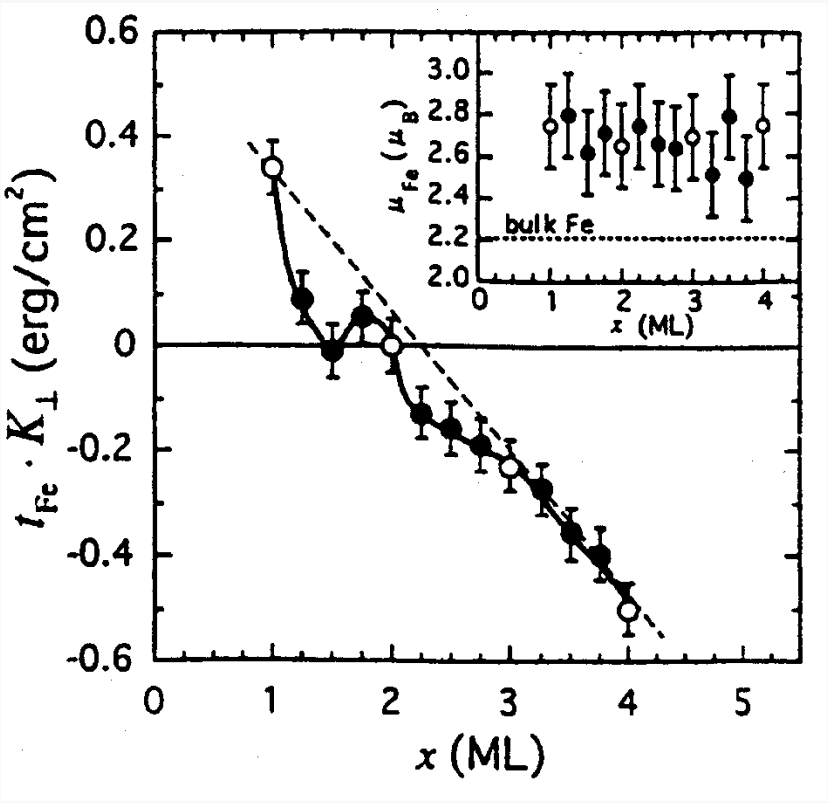

(7) Magneto-optical Kerr effect

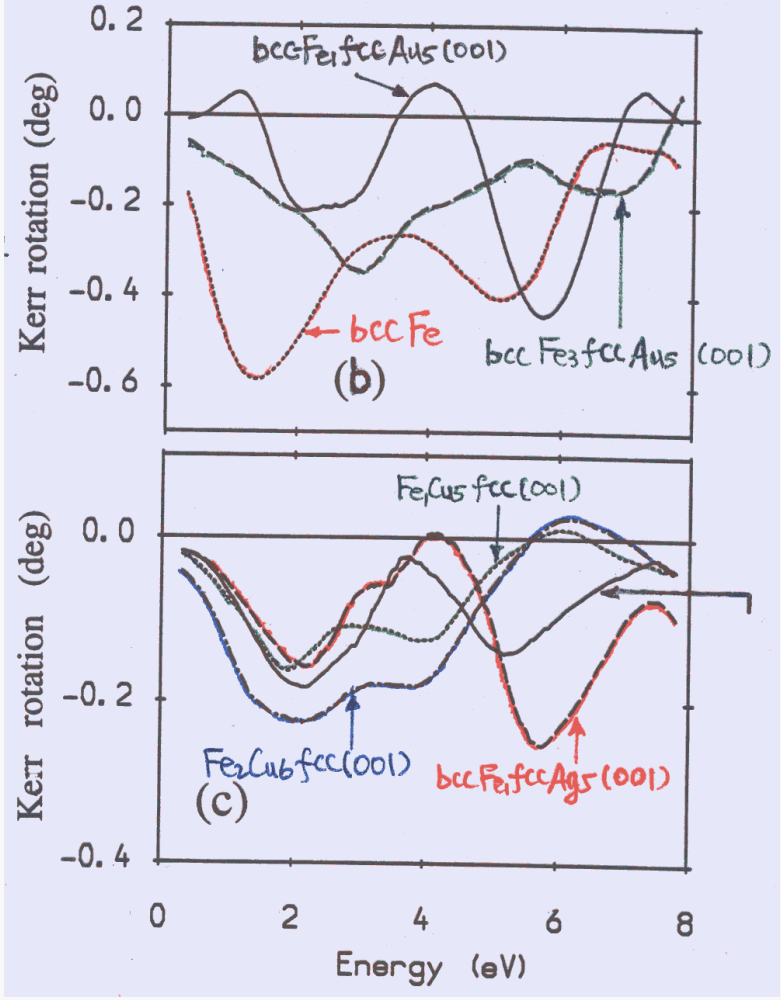

[Guo, Ebert, PRB 51 (1995) 12633]

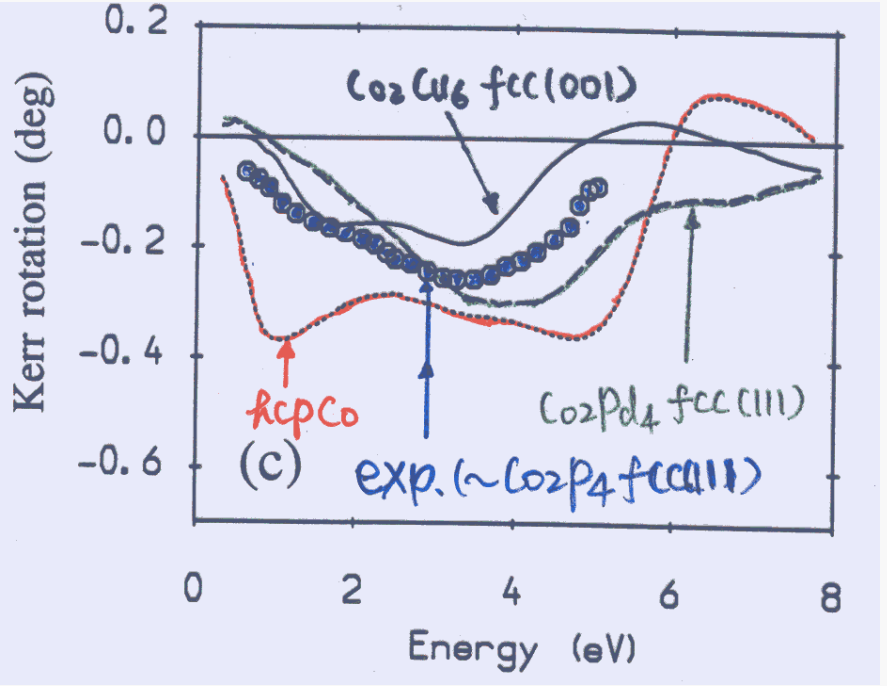

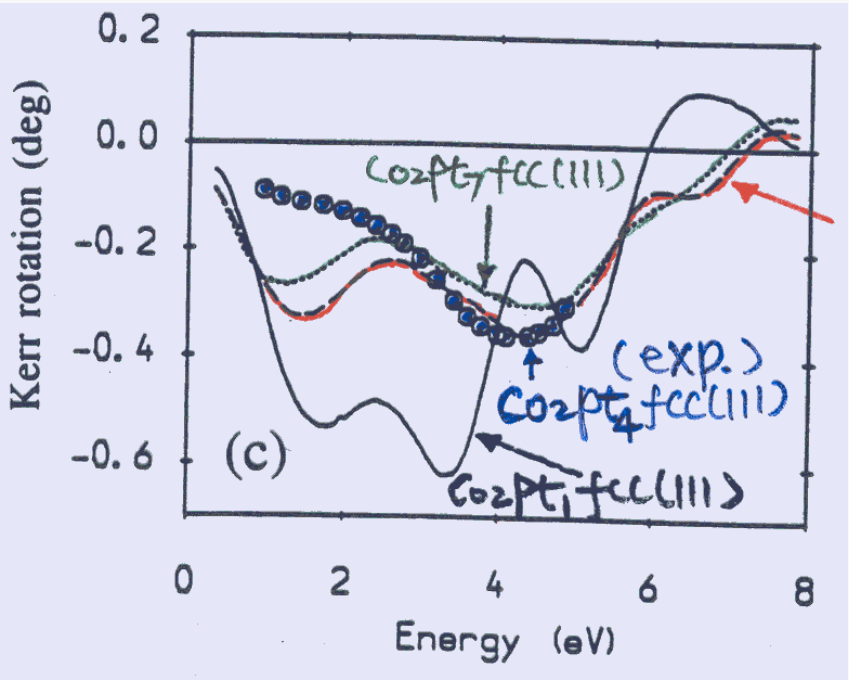

Origin of the enhanced Kerr effect in Pt multilayers?

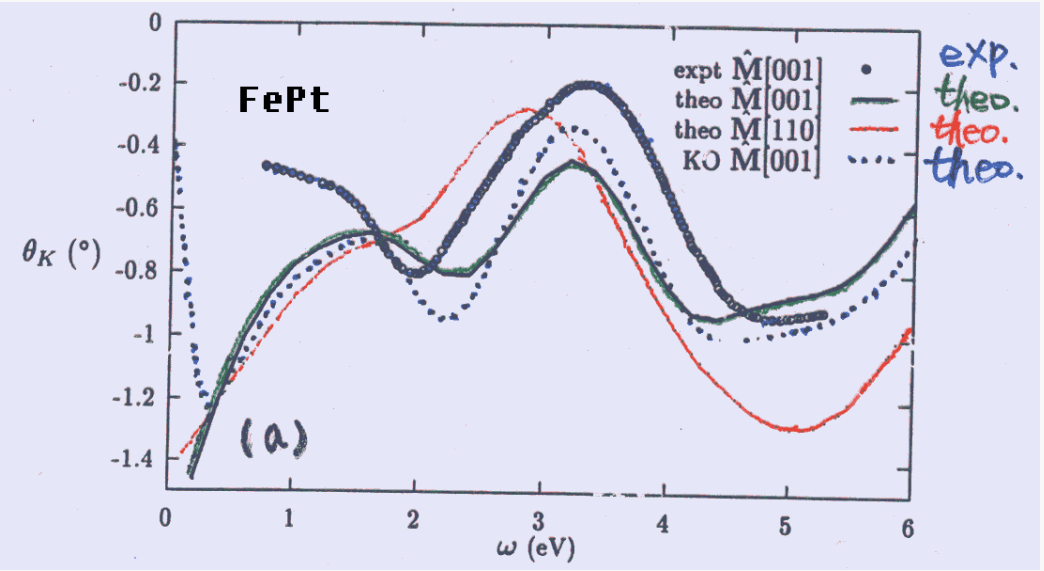

[Ebert, et al., IEEE 31 (1995) 3301]

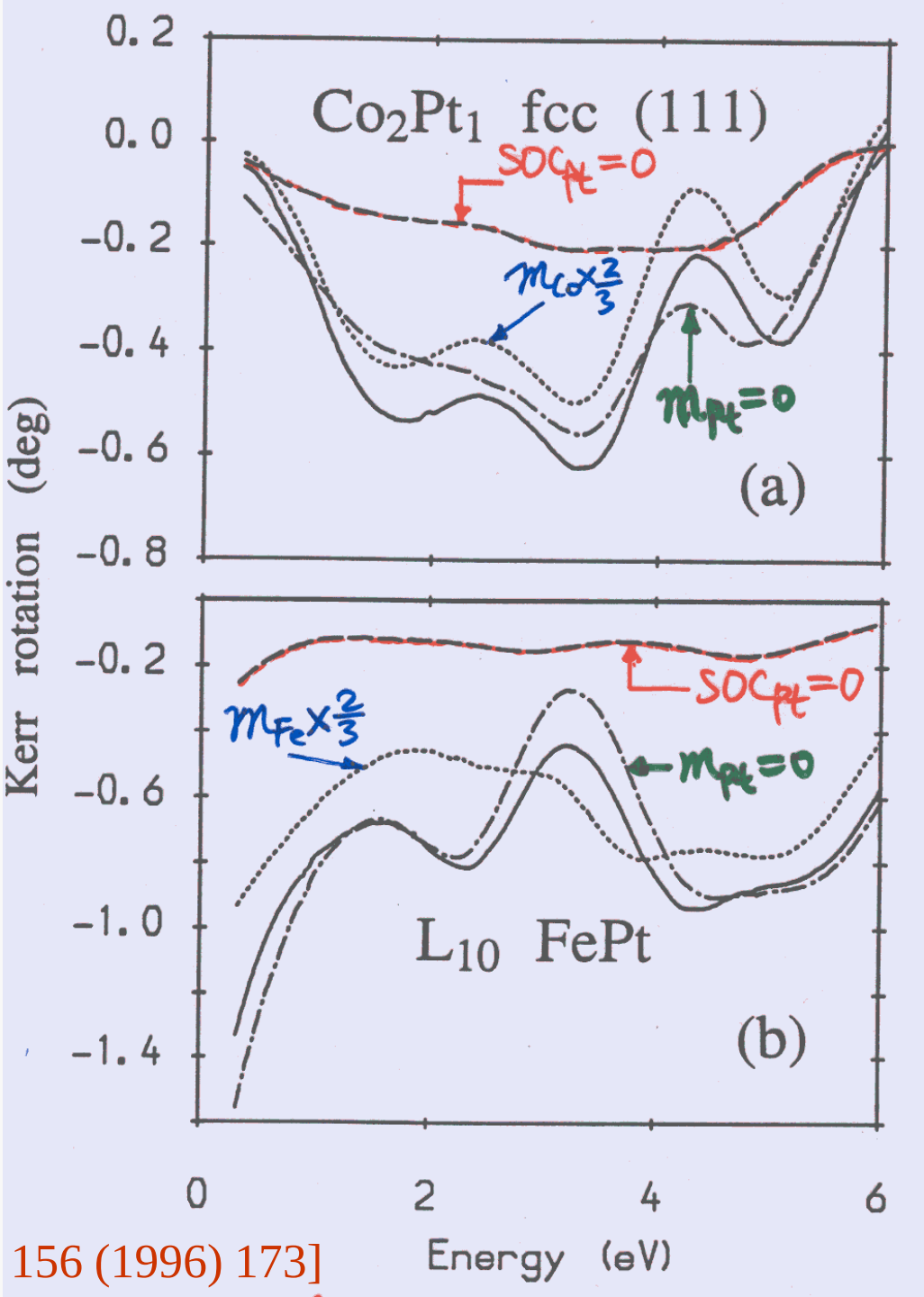

[Guo, Ebert, JMMM 156 (1996) 173]